DETERMINATION OF THE GRAVITY DISTURBANCE ON THE EARTH'S TOPOGRAPHIC SURFACE FROM AIRBORNE GRAVITY GRADIENT DATA

by

Yan Ming Wang

Report No. 401

Department of Geodetic Science and Surveying
The Ohio State University
Columbus, Ohio 43210-1247

December 1988

Abstract

The test flight of the gravity gradiometer survey system was taken in a flat area. In the future the tests will be carried out in rough mountain area and the topographic effect has to be taken into account. In this report the analytical downward continuation method was used to determine the gravity disturbance on the earth's topographic surface. The downward continuation is an improperly posed problem, especially in the processing of the aerial gradient data. In order to overcome this difficult, three methods were discussed and used for a simulated computation. The numerical computation shows that the gravity disturbance can be determined on the earth's surface with satisfactory accuracy. With a 1 Eötvös measurement error in the gravity gradient data, the gravity disturbance was determined on the earth's surface with the accuracy of 1 mgal. The gravity disturbance was recovered with the accuracy of 3 mgal when the measurement error of the gravity gradient was 5 Eötvös.

Foreword

This report was prepared by Wang Yan Ming, Research Associate, Department of Geodetic Science and Surveying at The Ohio State University. This research was sponsored by the Air Force Office of Scientific Research, Air Force Systems Command, Geophysics Laboratory, under Contract Number AFOSR F19628-86-K-0016, The Ohio State University Research Foundation Project 718188, project supervisor, Richard H. Rapp. The contract covering this research is administered by the Geophysics Laboratory, Hanscom Air Force Base, Massachusetts, with Dr. Christopher Jekeli, Scientific Program Officer.

Computer resources were provided by contract funds and by the funds supplied by the Instruction and Research Computer Center, through the Department of Geodetic Science and Surveying.

The reproduction and distribution of this report were carried out with funds supplied by the Department of Geodetic Science and Surveying.

Acknowledgments

I am very grateful to Dr. Richard H. Rapp for his suggestion of this research project. I wish to thank Dr. Christopher Jekeli for his valuable comments and suggestions. I also thank Ms. Lisa Schneck for the typing of this report.

Table of Contents

1. Introduction

After many years of development of the hardware, the airborne gravity gradiometry has reached the operational stage. The test flight was taken in the Texas-Oklahoma area and the test results were published (Brzezowski, et al., 1988). The test area is very smooth, so the topographic effect was neglected. In the future, the airborne gravity gradiometry will be used for the rough mountain area. The effect of the topography has to be taken into account in more rugged topographic areas. For many years this problem has been studied by different authors (Chinnery, 1961; Dorman et al., 1974; Hammer, 1976; Tziavos, et al., 1988). All studies had a basic idea - they intended to eliminate the effect of the topography by removing the mass above the geoid. The gradients of the attractions of the mass above the geoid were subtracted from the aerial gradient data, and the gravity disturbances could be determined on the geoid by processing the reduced aerial gradient data.

If the gravity disturbance is determined on the earth's surface, other methods can be used. One of the methods was suggested by Jekeli (1987). He used a surface integral to determine the disturbing potential on the earth's surface and avoided using the topographic reduction. Theoretically, this method is perfect but it is difficult to realize in practice, because the inclination of the topography, which is ill-defined, is needed at every computation point.

An alternative solution (ibid., p.239) which is difficult but simply defined is the use of the analytical continuation method. Assume that the derivatives of the disturbing potential T, such as T_z, T_{zz}, T_{zzz}, ..., can be well determined at a mean plane through the topographic surface. By analytical downward continuation, the gravity disturbance can be determined on the topographic surface by using Taylor's series.

It was shown (Schwarz, 1979; Rummel, et al., 1979; Neyman, 1985; Ilk, 1988) that downward continuation is an improperly posed problem. An improperly posed problem may have a solution but it does not depend on the data continuously. A small error in data, e.g. a random measurement error, can cause a significant deviation in the solution. It is expected that the second derivatives of the disturbing potential T, such as T_{zz}, T_{zx}, T_{xy}, ..., are rough at the flight altitude. The problem is, how can we downward continue these rough functions to a mean level? Furthermore, how can we absorb the useful information from such data to determine even higher derivatives of the disturbing potential on the mean level? Sometimes it looks like it is impossible, but if the gradient data is accurate and in good distribution, the reasonable results can always be expected. In order to avoid the instability of the computations and get a reasonable smooth solution, there are different methods that can be used, e.g., least squares collocation, regularization, or smoothing (filtering). These methods have the same property: they filter out the high frequency of the data and make the results stable and smooth. We will show that the three methods are identical under some conditions .

The goal of this study is to find methods for the determination of the gravity disturbance on the topographic surface by processing the aerial gradient data. The numerical computation will be carried out to gain an idea about the use of the methods.

Because the gradient data can be obtained at regular grid points, the very efficient numerical computation method - Fast Fourier transformation (FFT), is used. We will study the problem in the spectral domain and use FFT in the numerical computations.

2. Solution of the Analytical Downward Continuation for the Airborne Gravity Gradiometry

This section presents the formulas of the analytical downward continuation for the airborne gravity gradiometry.

Because the airbonre gravity-gradiometry is taken in a local area, the flat-earth approximation is suitable for the processing the aerial gravity gradient data (Jekeli, 1985).

At first we consider the analytical downward continuation of the aerial gravity-gradient data to the mean elevation level. The geometry of the airborne gravity-gradiometry is drawn in Figure 1.

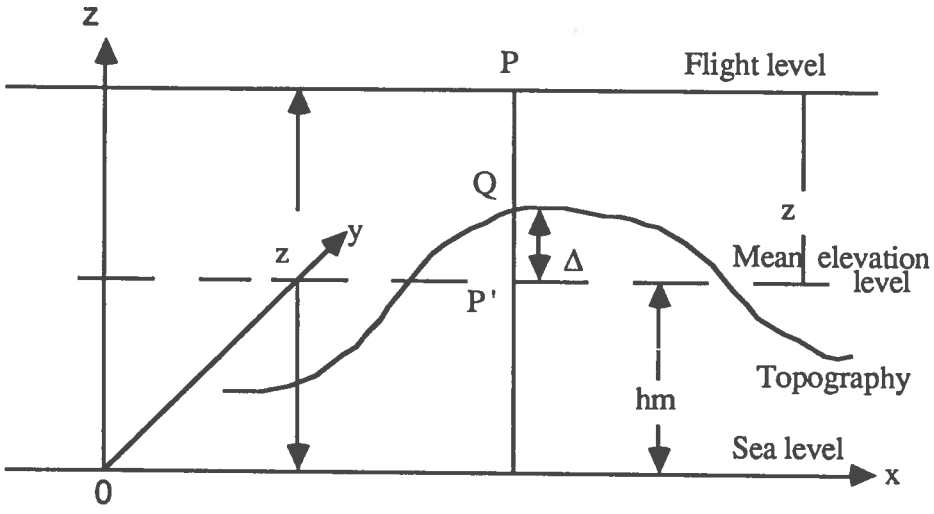

Figure 1. Geometry of the Airborne Gradiometry

Assume that the Runge's theorem (Moritz, 1980, p. 67) is valid also for the plane approximation, one can say that there is a function which is harmonic on and outside the mean elevation level and this function approximates the disturbing potential on and outside the earth's surface as good as we wish. We assume this function can be approximated by the analytically downward continuing the disturbing potential of the earth from outside the earth's surface to the mean elevation level.

Therefore we assume that the disturbing potential T and its derivatives, such as T_i, T_{ij}, i, j = 1, 2, 3 corresponding to the subscripts x, y, z respectively, are analytically downward continued inside the earth and are harmonic above the mean elevation level.

The Poisson's integral gives the relationship between a solid harmonic function and its values at the mean elevation level (cf. Heiskannen and Moritz, 1967, p. 239):

$$T(x_p, y_p, z_H) = \frac{z_H}{2\pi} \iint_{\tau} \frac{T(x, y)}{l^3} dx\, dy \qquad (1)$$

where $l = [(x-x_p)^2 + (y-y_p)^2 + z_H^2]^{1/2}$, is the distance between the current point on the mean elevation level τ and the point P at the flight level; z_H is the height of the flight level above the mean elevation level. Eq. (1) is valid for any harmonic function. For the derivatives of the disturbing potential T_i, T_{ij} we have:

$$T_i(x_p, y_p, z_H) = \frac{z_H}{2\pi} \iint_\tau \frac{T_i(x, y)}{l^3} dx\, dy \tag{2}$$

$$T_{ij}(x_p, y_p, z_H) = \frac{z_H}{2\pi} \iint_\tau \frac{T_{ij}(x, y)}{l^3} dx\, dy \qquad i, j = 1, 2, 3 \tag{3}$$

The second derivatives of the disturbing potential T_{ij} are given on the flight level, the derivatives of the disturbing potential T, such as T_i, T_{iz}, T_{izz} and even higher terms will be determined on the mean elevation level. We consider this process in two steps: first the components of the gravity disturbance T_i are computed at the flight level by processing the second derivatives of the disturbing potential T_{ij}. The formulas can be found in (Jekeli, 1985)

$$T_z(x, y) = -\frac{1}{2\pi} \iint_{-\infty}^{\infty} \frac{T_{zz}(x', y')}{l_0} dx'\, dy' \tag{4}$$

$$T_x(x, y) = -\frac{1}{2\pi} \iint_{-\infty}^{\infty} \frac{T_{xz}(x', y')}{l_0} dx'\, dy' \tag{5}$$

$$T_y(x, y) = -\frac{1}{2\pi} \iint_{-\infty}^{\infty} \frac{T_{yz}(x', y')}{l_0} dx'\, dy' \tag{6}$$

$$T_x(x, y) = \frac{1}{2\pi} \iint_{-\infty}^{\infty} \frac{T_{zz}(x', y')}{l_0} \sin\alpha\, dx'\, dy' \tag{7}$$

$$T_y(x, y) = \frac{1}{2\pi} \iint_{-\infty}^{\infty} \frac{T_{zz}(x', y')}{l_0} \cos\alpha\, dx'\, dy' \tag{8}$$

where $l_0^2 = (x-x')^2 + (y-y')^2$ and α is the azimuth of the point (x', y') with respect to the point (x,y).

The second step is to downward continue the derivatives of the disturbing potential T_i, T_{iz}, T_{izz} to the mean level by using the Poisson's integral. If T_i, T_{iz}, T_{izz} are determined on the mean level, then we can get the gravity disturbance on the topographic surface by using Taylor's series:

$$T_i(Q) = T_i(P') + \Delta h \left.\frac{\partial T_i}{\partial h}\right|_{h=hm} + \frac{1}{2}(\Delta h)^2 \left.\frac{\partial^2 T_i}{\partial h^2}\right|_{h=hm}$$

$$= T_i(P') + \Delta h\, T_{iz}(P') + \frac{1}{2}(\Delta h)^2 T_{izz}(P') \qquad i = 1, 2, 3 \tag{9}$$

where $\Delta h = \overline{QP'} = h_Q - h_m$, the height of the topography referenced to the mean elevation level.

The role of the mean elevation level is like the point level in the analytical downward continuation solution of the Molodensky's problem (Moritz, 1980). Instead of the point level in the solution of the Molodensky's problem the mean elevation level is being used, so that T_i, Δh T_{iz}, $1/2\ (\Delta h)^2\ T_{izz}$ should have a similar magnitude and property as Δg, g_1 and g_2 of the solution of the Molodensky's problem. For more details about the numerical properties of g_1, g_2 and higher terms see (Wang, 1987).

In the following discussion we consider how the gravity disturbance and its derivatives can best be determined on the mean elevation level. First we consider the use of least squares collocation to process the aerial gravity-gradient data.

3. Processing the Aerial Gravity-Gradient Data by Using Least Squares Collocation in a Continuous Case

If the data are dense and regularly distributed as in the case of airborne gradiometry, least squares collocation can be considered in a continuous case. The advantages are that the problem can be solved in the frequency domain easily and the efficient numerical computation method - Fast Fourier transform can be used.

Generally, we consider the operator equation

$$g^\circ = Af \qquad g^\circ \in G, \quad f \in F \tag{10}$$

where A: $F \rightarrow G$, a linear operator which maps the normed space F into the normed space G. In airborne gradiometry A can be any integral or differential operator. A specific example is: A is the upward continue operator defined by the Poisson's integral (formula (3)); f is the second derivative of the disturbing potential T_{ij} at the mean level τ and g° is T_{ij} at the flight level. Now we have the second derivatives of the disturbing potential T_{ij} at the flight level. We want to determine T_{ij} on the mean level τ. This inverse problem may be properly posed if T_{ij} at the flight level is smooth enough and errorless.

In practice such an inverse problem is improperly defined, because we always have the errors in the data. It means, instead of the original function g°, we have in practice

$$g = g^\circ + \varepsilon \tag{11}$$

where ε is the measurement error.

Even though the inverse of the operator A^{-1} exists, the solution

$$f^* = A^{-1} g \tag{12}$$

can be quite different from f which we are trying to determine. Now we want to find the methods to overcome this difficulty.

If we have the previous information about the statistics of the data and the measurement error, the method of least squares collocation can be used to obtain a solution. This technique has become a standard computational method for the inverse problem in physical geodesy.

In eq. (11) we assume that the function g° is centered:

$$M\{g^\circ\} = 0$$

The operator M is defined as

$$M\{g^\circ\} = \lim_{T\to\infty} \frac{1}{4T^2} \int_{-T}^{T} \int_{-T}^{T} g^\circ(x, y)\, dx\, dy \tag{13}$$

The function g° is deterministic and the error ε is considered as a stochastic process, so the measurement g is a stochastic process.

The variance and the covariance function are defined as

$$C_{ff}(P, Q) = M\{f(P) f(Q)\}$$
$$C_{fg}(P, Q) = M\{f(P) g(Q)\} \tag{14}$$

P, Q are the points on the reference plane.

We assume the function g° and the error ε are independent:

$$M\{\varepsilon(P) g^\circ(Q)\} = M\{g^\circ(P) \varepsilon(Q)\} = 0$$
$$M\{\varepsilon(P) g(Q)\} = M\{\varepsilon(P) \varepsilon(Q)\} = C_{nn}(P,Q) \tag{15}$$

where C_{nn} is the covariance of the error ε.

We consider a process for the best estimation of the function f:

$$\hat{f} = Hg \tag{16}$$

where $\hat{f}$ is the best estimate of the function f, H is the estimation operator which makes the mean square estimation error e the smallest:

$$M\{e^2\} = M\{(f-\hat{f})^2\} = \text{min.} \tag{17}$$

Eq. (17) is equivalent to

$$C_{ee}(r = 0, H) = \text{min.} \tag{18}$$

where C_{ee} is the covariance of the estimation error, and it is a function of the estimator H; r is the distance between the points P and Q.

Eq. (18) can be viewed as an extreme value problem: To find an estimator H which makes C_{ee} (r = 0, H) the smallest.

Now we consider how to solve this minimum problem in the frequency domain.

The two dimensional Fourier transformation and its inverse are defined by

$$F\{f(x,y)\} = \int\int_{-\infty}^{\infty} f(x,y)\, e^{2\pi j(xu+yv)}\, dx\, dy \tag{19}$$

$$F^{-1}\{g(u,v)\} = \int\int_{-\infty}^{\infty} g(u,v)\, e^{-2\pi j(xu+yv)}\, du\, dv \tag{20}$$

where $j = \sqrt{-1}$; F and F^{-1} denote the Fourier transformation and its inverse respectively.

We denote the Fourier transformation of the function f by ω_f

$$\omega_f = F\{f(x, y)\} \tag{21}$$

and assume that

$$F\{Af\} = \phi_A\, \omega_f \tag{22}$$

$$F\{Hf\} = \phi_H\, \omega_f$$

where ϕ_A, ϕ_H are called the spectra of the operators A and H respectively.

For the Fourier transformation of the covariances we have (cf. Schwarz, et al., 1989):

$$R_{ff}(u,v) = F\{C_{ff}(x,y)\} = \lim_{T\to\infty} \frac{1}{4T^2}\left(\omega_f \omega_f^*\right) \tag{23}$$

$$R_{fg}(u,v) = F\{C_{fg}(x,y)\} = \lim_{T\to\infty} \frac{1}{4T^2}\left(\omega_f \omega_g^*\right)$$

$$= \lim_{T\to\infty} \frac{1}{4T^2}\left(\omega_f \phi_A^* \omega_f^*\right) = \phi_A^* R_{ff} \tag{24}$$

$$R_{gf}(u, v) = F\{C_{gf}(x, y)\} = \phi_A\, R_{ff}$$

$$= R_{fg}^* \tag{25}$$

$$R_{gg}(u, v) = \phi_A\, \phi_A^*\, R_{ff} \tag{26}$$

where the symbol " * " denotes the conjugate of a complex function and R_{ff}, R_{fg}, R_{gf}, R_{gg} are the Fourier transformation of the covariances. Sometimes they are called the power spectral density function.

If we denote the power spectral density of the estimation error by R_{ee} (u, v), then eq. (18) can be written in the form:

$$C_{ee}(r = 0, H) = \int\int_{-\infty}^{\infty} R_{ee}(u, v, \phi_H)\, du\, dv = \min . \tag{27}$$

then the extreme value problem becomes:

To find the spectrum of the operator H which makes the estimation error the smallest.

If there is a procedure which minimizes the power spectral density function of the estimation error everywhere in the frequency domain:

$$R_{ee}(u, v, \phi_H) = \min., \qquad u, v \in (-\infty, +\infty) \tag{28}$$

the word "everywhere" means the minimum values of R_{ee} for every frequency u, v, then the extreme value problem (18) can be replaced by (28) in frequency domain. The minimum condition (28) was used by Bendat (1980) for minimizing the power spectral density function of the estimation error.

Note that the R_{ee} is non-negative and compare eq. (28) with eq. (27), one can find that eq. (27) can be obtained by using eq. (28). If the power spectral density function R_{ee} is minimized everywhere, its integration C_{ee} (r = 0, H) is also smallest.

The estimation error covariance is given by

$$C_{ee} = M\{e(P)\, e(Q)\} = M\left\{\left[f(P) - \hat{f}(P)\right]\left[f(Q) - \hat{f}(Q)\right]\right\},$$

$$= C_{ff} - C_{ff\hat{}} - C_{f\hat{}f} + C_{\hat{f}\hat{f}} \tag{29}$$

Using eqs. (23) - (26) and (29) we get the power spectral density function of the estimation error e:

$$R_{ee} = R_{ff} - \phi_H^* \phi_A^* R_{ff} - \phi_H \phi_A R_{ff} + \phi_H \phi_H^* \left(\phi_A \phi_A^* R_{ff} + R_{nn}\right) \tag{30}$$

Under the minimum condition (28), the spectra ϕ_H^*, ϕ_H have to satisfy the following conditions:

$$\frac{\partial}{\partial \phi_H^*}(R_{ee}) = 0 \tag{31}$$

$$\frac{\partial}{\partial \phi_H}(R_{ee}) = 0$$

From (30) and (31) we get:

$$\phi_H = \frac{\overset{*}{\phi}_A R_{ff}}{\overset{*}{\phi}_A \phi_A R_{ff} + R_{nn}} \tag{32}$$

$$\overset{*}{\phi}_H = \frac{\phi_A R_{ff}}{\overset{*}{\phi}_A \phi_A R_{ff} + R_{nn}} \tag{33}$$

The best estimate of the function f is given by

$$\hat{f} = F^{-1}\left\{\phi_H \omega_g\right\}$$

$$= F^{-1}\left\{\frac{\overset{*}{\phi}_A R_{ff}}{\overset{*}{\phi}_A \phi_A R_{ff} + R_{nn}} \omega_g\right\} \tag{34}$$

where ω_g is the Fourier transformation of the measurement (data) g.

The estimation error is given by (cf. eqs. (27) and (30)):

$$M\{e^2\} = C_{ee}(0)$$

$$= \int\int_{-\infty}^{\infty}\left[\left(1 - \phi_A \phi_H\right)^2 R_{ff} + \phi_H \overset{*}{\phi}_H R_{nn}\right] dudv \tag{35}$$

If the pre-information of the statistics of the function f and the error e, or the power spectral density function R_{ff} and R_{nn}, are known, then we can use formulas (32) and (34) to get the best estimation of the function f from the data g. The estimation error can be computed by using eq. (35).

Now we consider a more general case. We have a heterogeneous data set related to the function f:

$$
\begin{aligned}
g_1 &= A_1 f + \varepsilon_1 \\
g_2 &= A_2 f + \varepsilon_2 \\
&\cdot \\
&\cdot \\
&\cdot \\
g_n &= A_n f + \varepsilon_n ,
\end{aligned}
\tag{36}
$$

A solution which is the best approximation of the function f is to be determined by processing this heterogeneous data. An example for eq. (36) is the processing of aerial gravity-gradient data. g_i, i = 1, 2, ... 6 is the second derivative of the disturbing potential, and f can be the disturbing potential or any of its derivatives. Of course, if we have any other data related to the function f, we can always put it in the form as eq. (36).

We assume the best estimate of the function f is given by:

$$
\hat{f} = H_1 g_1 + H_2 g_2 + \ldots + H_n g_n = \sum_{i=1}^{n} H_i g_i \tag{37}
$$

The estimation error is

$$
e = f - \hat{f} = f - \sum_{i=1}^{n} H_i g_i \tag{38}
$$

The estimation error covariance has the same form as eq. (29):

$$
C_{ee} = C_{ff} - C_{ff}^{\wedge} - C_{ff}^{\wedge} + C_{ff}^{\wedge\wedge} \tag{29'}
$$

Note that

$$
\begin{aligned}
R_{\hat{f}\hat{f}} &= F\{C_{\hat{f}\hat{f}}\} = \lim_{T\to\infty} \frac{1}{4T^2}\left(\omega_f \omega_f^*\right) \\
&= \sum_{i=1}^{n} \phi_{H_i} \phi_i R_{ff} \\
R_{ff}^{\wedge} &= F\{C_{ff}^{\wedge}\} \\
&= \sum_{j=1}^{n} \phi_{H_j}^{*} \phi_j^{*} R_{ff} \\
R_{ff}^{\wedge\wedge} &= F\{C_{ff}^{\wedge\wedge}\}
\end{aligned}
\tag{39}
$$

$$= \sum_{i=1}^{n} \sum_{j=1}^{n} \phi_{H_i} \overset{*}{\phi}_{H_j} \left(\phi_i \overset{*}{\phi}_j R_{ff} + R_{ij} \right),$$

where

$$R_{ij} = \begin{cases} R_{jj} \neq 0 & i=j \\ 0 & i \neq j \end{cases}, \tag{40}$$

Here we have assumed the measure errors ε_i, i = 1, 2, ... n are independent of each other; R_{jj} is the power spectral density function of the measurement error ε_j; ϕ_i is the spectrum of the operator A_i. The spectral density function of the estimation error is:

$$R_{ee} = R_{ff} - \sum_{i=1}^{n} \phi_{H_i} \phi_i R_{ff} - \sum_{j=1}^{n} \overset{*}{\phi}_{H_j} \overset{*}{\phi}_j R_{ff} +$$

$$+ \sum_{i=1}^{n} \sum_{j=1}^{n} \phi_{H_i} \overset{*}{\phi}_{H_j} \left(\phi_i \overset{*}{\phi}_j R_{ff} + R_{ij} \right) \tag{41}$$

The power spectral density function R_{ee} has the extreme value when:

$$\frac{\partial R_{ee}}{\partial \overset{*}{\phi}_{H_j}} = 0$$

$$\frac{\partial R_{ee}}{\partial \phi_{H_i}} = 0 \tag{42}$$

Using eqs. (41) and (42) we get

$$- \sum_{j=1}^{n} \overset{*}{\phi}_j R_{ff} + \sum_{i=1}^{n} \sum_{j=1}^{n} \phi_{H_i} \left(\phi_i \overset{*}{\phi}_j R_{ff} + R_{ij} \right) = 0$$

$$- \sum_{i=1}^{n} \phi_i R_{ff} + \sum_{i=1}^{n} \sum_{j=1}^{n} \overset{*}{\phi}_{H_j} \left(\phi_i \overset{*}{\phi}_j R_{ff} + R_{ij} \right) = 0 \tag{43}$$

Eq. (43) can be rewritten as

$$\sum_{j=1}^{n} \left[- \overset{*}{\phi}_j R_{ff} + \sum_{i=1}^{n} \phi_{H_i} \left(\phi_i \overset{*}{\phi}_j R_{ff} + R_{ij} \right) \right] = 0 \tag{43*}$$

$$\sum_{i=1}^{n}\left[-\overset{*}{\phi}_i R_{ff}+\sum_{j=1}^{n}\overset{*}{\phi}_{H_j}\left(\phi_i\overset{*}{\phi}_j R_{ff}+R_{ij}\right)\right]=0$$

Eq. (43*) implies that

$$-\overset{*}{\phi}_j R_{ff}+\sum_{i=1}^{n}\phi_{H_i}\left(\phi_i\overset{*}{\phi}_j R_{ff}+R_{ij}\right)=0 \tag{44}$$

$$-\phi_i R_{ff}+\sum_{j=1}^{n}\overset{*}{\phi}_{H_i}\left(\phi_i\overset{*}{\phi}_j R_{ff}+R_{ij}\right)=0 \tag{45}$$

Equations (44) and (45) are conjugate to each other. They are indeterminate linear equations. There are infinite solutions for the "variables" ϕ_{H_i} and $\overset{*}{\phi}_{Hj}$. One of the solutions of eq. (44) can be written as:

$$\phi_{H_i}=\frac{\overset{*}{\phi}_i R_{ff}}{\sum_{j=1}^{n}\phi_j\overset{*}{\phi}_j R_{ff}+R_{ii}} \qquad \text{when } R_{11}=R_{22}=\ldots R_{nn} \tag{46}$$

This is a special case in which all measurement errors have the same magnitude and property (same power spectral density function). One can expect that it can happen sometimes, e.g., in the airborne gravity-gradiometry, the components of the gradient of the gravity are measured with different accuracy.

In the last case the solution for the indeterminate equation (44) can be

$$\phi_{H_i}=\frac{\overset{*}{\phi}_i R_{ff}R_{ii}^{-1}}{\sum_{j=1}^{n}\overset{*}{\phi}_j\phi_j R_{ff}R_{jj}^{-1}+1} \tag{47}$$

If the power spectral density function of the measurement error is "white" noise, we have:

$$R_{ii}=\text{constant} \tag{48}$$

We then can define a spectral weight ω_p^i by

$$\omega_p^i = R_{ii}^{-1} \tag{49}$$

so that equation (47) becomes:

$$\phi_{H_i} = \frac{\phi_i^* R_{ff} \omega_p^i}{\sum_{j=1}^{n} \phi_j^* \phi_j R_{ff} \omega_p^j + 1} \tag{50}$$

Obviously, eq. (50) can be considered as a weighted least squares collocation solution with weight ω_p^i. If a data set is measured with low accuracy, based on eqs. (49) and (50), the spectral weight ω_p^i becomes smaller and so the ϕ_{H_i}. This data set is weighted and has less contribution to the results.

The definition of the spectral weight ω_p^i can also be expanded to a more general case in which the R_{ee} is not restricted to be a constant. Assume that the power spectral density function of the measurement errors is not only the "white" noise and let eq. (49) still be valid, eq. (47) can be considered as a weighted least squares collocation solution with weight ω_p^i, too. The only difference from the "white" noise case is that the spectral weight ω_p^i has different values to different frequencies.

We now consider only the case in which all data are measured with the same accuracy. The best estimation of the function f is given by

$$\hat{f} = F^{-1}\left\{\sum_{i=1}^{n} \phi_{H_i} \omega_{g_i}\right\}$$

$$= F^{-1}\left\{\sum_{i=1}^{n} \frac{\phi_i^* \omega_{g_i} R_{ff}}{\sum_{j=1}^{n} \phi_j \phi_j^* R_{ff} + R_{ii}}\right\} \tag{51}$$

where ω_{g_i} is the Fourier transform of the data g_i.

The estimation error variance is (cf. eqs. (27) and (41)):

$$M\{e^2\} = C_{ee}(0)$$

$$= \int\int_{-\infty}^{\infty} \left[\left(1 - \sum_{i=1}^{n} \phi_i \phi_{H_i}\right)^2 R_{ff} + \sum_{i=1}^{n} \left|\phi_{H_i}\right|^2 R_{ii}\right] dudv \tag{52}$$

Here we have used:

$$\sum_{i=1}^{n}\sum_{j=1}^{n}\phi_{H_i}\overset{*}{\phi}_{H_j}R_{ij}=\sum_{j=1}^{n}\phi_{H_i}\overset{*}{\phi}_{H_i}R_{ii} \tag{53}$$

In an ideal case the data are errorless, the spectrum of the best estimation operator H_i has the form:

$$\phi_{H_i}=\frac{\overset{*}{\phi}_i}{\sum_{i=1}^{n}\phi_i\overset{*}{\phi}_i}, \tag{54}$$

then the function f can be exactly recovered without using any pre-information of the statistics of the function f.

Because eqs. (44), and (45) are indeterminate linear equations and pose infinite solutions, we can find another solutions of the operator H_i which satisfies eqs. (44) and (45). An alternative method to solve this problem is discussed in (Bendat, et al., 1980, Chapter 10).

The above formulas can be used for any observed quantities which are related to the disturbing potential, e.g., the gravity anomalies; deflections of the vertical; geoid undulation etc. If we have such heterogeneous data, the above formulas can be used to determine the needed quantities.

The weakness of this method is that the data have to be regularly distributed and should not be so sparse that the interested information is lost.

4. Regularization

In Section 3 we have considered the solution of the improperly posed problem by using least squares collocation. Now we study the problem from another starting point. We will consider the solution to be stable and smooth.

In least squares collocation the statistics of the determined function and the measurement error have to be known. In practice, they are never exactly known and are always assumed. If the solutions are sensitive to the statistical model of the measurement error or of the function being estimated, or the statistical model is not properly assumed, the results may not be good or not stable. In this case one can consider the use of a regularization method.

The regularization method has been used in many technical and scientific areas (Nashed, 1974). The use of the regularization in physical geodesy can be found in (Schwarz, 1979; Neyman, 1985; Ilk, 1988). This method is flexible in obtaining a stable and smooth solution because we have the chance to choose the regularization parameter and the regularization function arbitrarily.

There are different regularization methods and different ways to regularize an improperly posed problem; for more detailed see Nashed (1974). Here we are interested in this problem: Find a solution where its n^{th} derivatives are smooth and it is the best approximation of the original solution.

For the improperly posed operator equation

$$g = Af \tag{10'}$$

$$f \in F, g \in G$$

Let F, G and Z be Hilbert spaces and A: F→G be an operator mapping the Hilbert space F into G; L_m: F→Z be an operator mapping the Hilbert space F into Z. We consider the minimization problem: find a function f_α to minimize the functional

$$J\left(f, g, \alpha, L_m\right) = \|Af - g\|_G^2 + \alpha^2 \|L_m f\|_Z \tag{55}$$

where the norm of a function f is defined

$$\|f\|^2 = (f, f) \tag{56}$$

Eq. (56) is from the definition of the Hilbert space (Bachman, et al., 1966, p. 141). The inner product (f, f) can be defined for our purpose as:

$$(f,f) = \lim_{T\to\infty} \frac{1}{4T^2} \int_{-T}^{T} \int_{-T}^{T} f f^* dx\, dy \tag{57}$$

where f* is the conjugate of the function f.

Notice that

$$Af - g = \varepsilon \tag{58}$$

where ε is the measurement error, therefore eq. (55) is equal to

$$J\left(f, g, \alpha, L_m\right) = \left\|\varepsilon\right\|_G^2 + \alpha^2 \|L_m f\|_Z \tag{59}$$

Let $\alpha = 0$, then the minimization problem (55) becomes: find a function f_α to minimize the functional

$$J(f, g) = \left\|\varepsilon\right\|_G^2 \tag{60}$$

Eq. (60) is a classic least-squares minimization problem. The physical meaning of the last term in (59) is clear. If L_m is chosen as a differential operator up to m order, then the minimization

problem (55) means: to find a function f_α to minimize not only the measurement error, but also the functional $||L_m f||$. The last term $||L_m f||$ makes the function f_α smooth and stable and it makes the difference between the classic least-squares minimization problem and the regularization problem.

The solution of (55) has been given by (Nashed, 1974, chapter 4):

$$\left(A^* A + \alpha^2 L_m^* L_m\right) f_\alpha = A^* g \tag{61}$$

where A* is the adjoint operator and is defined by (Bachman, et al., 1966, p. 16):

$$(Ax, y) = (x, A^* y), \quad x, y \in F \tag{62}$$

If the inverse of the operator

$$\left(A^* A + \alpha^2 L_m^* L_m\right)$$

exists, then we have the solution

$$f_\alpha = \left(A^* A + \alpha L_m^* L_m\right)^{-1} A^* g \tag{63}$$

Based on the Lemma 2.2 (ibid, p. 25) we get the spectrum of the adjoint operator A*:

$$\phi_{A^*} = \overset{*}{\phi}_A \tag{64}$$

That means that the spectrum of the adjoint operator A* is equal to the conjugate of the spectrum of the operator A.

Applying the Fourier transformation to eq. (61), we get the spectrum of the regularization solution f_α:

$$F\{f_\alpha\} = \omega_{f_\alpha} = \frac{\overset{*}{\phi}_A \omega_g}{\overset{*}{\phi}_A \phi_A + \alpha^2 \overset{*}{\phi}_{L_m} \phi_{L_m}} \tag{65}$$

We denote (61) by an operator equation

$$f_\alpha = H_0 g \tag{66}$$

with

$$H_0 = \left(A^* A + \alpha^2 L_m^* L_m\right)^{-1} A^* \tag{67}$$

H_0 was viewed as a regularization operator by Nashed (1974).

In the spectral domain eq. (66) can be written in the form (cf. eq. (65)):

$$\omega_{f_\alpha} = \phi_{H_0} \omega_g \tag{68}$$

with

$$\phi_{H_0} = \frac{\overset{*}{\phi}_A}{\overset{*}{\phi}_A \phi_A + \alpha^2 \overset{*}{\phi}_{L_m} \phi_{L_m}} \tag{69}$$

The regularization error is defined as

$$e^r = f - f_\alpha \,, \tag{70}$$

and the error covariance is

$$\begin{aligned} C_{ee}^r &= M\left\{e^r(P)\, e^r(Q)\right\} \\ &= C_{ff} - C_{f\alpha f} - C_{ff\alpha} + C_{f\alpha f\alpha} \end{aligned} \tag{71}$$

The power spectral density function of the regularization error is given by:

$$\begin{aligned} R_{ee}^r(u, v) &= F\left\{C_{ee}^r(x, y)\right\} \\ &= \left(1 - \phi_{H_0}\phi_A\right)^2 R_{ff} + \left|\phi_{H_0}\right|^2 R_{nn} \end{aligned} \tag{72}$$

where R_{nn} is the power spectral density function of the measurement error.

From eqs. (61) and (69) we can see that the solution f_α is dependent on the regularization parameter α and on the choices of the operator L_m. No statistical model of the function f and the measurement error are needed. But if the regularization error is to be determined, the statistics of the measurement error and of the function being estimated, are always needed (cf. eq. (72)).

The mean square of the regularization error is given by:

$$C_{ee}^r(0, \alpha, L_m) = \int\int_{-\infty}^{\infty} R^r(u, v)\, du dv$$

$$= \int\int_{-\infty}^{\infty} \left[\left(1 - \phi_{H_0}\phi_A\right)^2 R_{ff} + \left|\phi_{H_q}\right|^2 R_{nn} \right] dudv \qquad (73)$$

$C^r_{ee}(0, \alpha, L_m)$ is a function of the regularization parameters α and the operator L_m.

The regularization of the improperly posed problem can be extended to the heterogeneous data. Denote the equations (36) with the vectorial form:

$$\underline{g} = \underline{A}\, f \qquad (74)$$

where the underbar denotes the vector, $\underline{g}$ is a vector function with the components g_i, i = 1, 2, ...n, and $\underline{A}$ is a vector operator with components A_i, i = 1, 2, ... n. The minimization problem is: Find a function f_α, to minimize the functional

$$J(f, \underline{g}, \alpha, L_m) = \| \underline{A}\, f - \underline{g} \|^2_G + \alpha^2 \|L_m f\|^2_Z \qquad (75)$$

The norm of a vector in the Hilbert space G is defined by the inner product:

$$\|g\|^2 = (\underline{g}, \underline{g}) = (\underline{A}f, \underline{A}f)$$

$$= (\underline{A}^+ \cdot \underline{A}f, f) \qquad (76)$$

where the symbol "+" denotes the transpose of the adjoint operator of the vector operator $\underline{A}$. The product of the $\underline{A}^+ \cdot \underline{A}$ is a scalar operator and it is given by

$$\underline{A}^+ \cdot \underline{A} = A_1^* A_1 + A_2^* A_2 + \ldots + A_n^* A_n \qquad (77)$$

Because the $\underline{A}f$, $\underline{g}$ are the elements of the Hilbert space G, therefore the extreme value problem (75) is the same as the problem defined in (ibid, chapter 4). The solution of eq. (75) is then

$$(\underline{A}^+ \cdot \underline{A} + \alpha^2 L_m^* L_m)\, f_\alpha = \underline{A}^+ \cdot \underline{g} \qquad (78)$$

If the inverse of the operator

$$\underline{A}^+ \cdot \underline{A} + \alpha^2 L_m^* L_m$$

exists, then eq. (78) can be written in the form

$$f_\alpha = (\underline{A}^+ \cdot \underline{A} + \alpha^2 L_m^* L_m)^{-1}\, \underline{A}^+ \cdot \underline{g} \qquad (79)$$

By using eq. (77) and the definition of the vector operator eq. (78) can be written as

$$\left(\sum_{i=1}^{n} A_i^* A_i + \alpha^2 L_m^* L_m \right) f_\alpha = \sum_{i=1}^{n} A_i^* g_i \qquad (80)$$

Applying the Fourier transformation to eq. (80) and using eqs. (22) and (64), we obtain the spectrum of the regularized function f_α:

$$\omega_{f_\alpha} = \frac{\sum_{i=1}^{n} \phi_i^* \omega_{g_i}}{\sum_{i=1}^{n} \phi_i^* \phi_i + \alpha^2 \phi_{L_m}^* \phi_{L_m}} \tag{81}$$

In order to get the f_α in space domain, the operator equation (80) has to be solved. In the frequency domain this problem becomes much easier: the regularized function f_α can be obtained by taking the inverse Fourier transformation of eq. (81).

The estimation error covariance is the same as eq. (71):

$$C_{ee}^R = C_{ff} - C_{f_\alpha f} - C_{ff_\alpha} + C_{f_\alpha f_\alpha} \tag{82}$$

where the superscript "R" distinguishes the estimation error covariance between the heterogenous data and the homogeneous data cases.

Notice that

$$\begin{aligned} F\{C_{ff}\} &= R_{ff} \\ F\{C_{f_\alpha f}\} &= \phi_0 R_{ff} \\ F\{C_{ff_\alpha}\} &= \phi_0^* R_{ff} \\ F\{C_{f_\alpha f_\alpha}\} &= \phi_0 \phi_0^* R_{ff} + \phi_e^2, \end{aligned} \tag{83}$$

where

$$\phi_0 = \phi_0^* = \frac{\sum_{i=1}^{n} \phi_i^* \phi_i}{\sum_{i=1}^{n} \phi_i^* \phi_i + \alpha^2 \phi_{L_m}^* \phi_{L_m}} \tag{84}$$

$$\phi_e^2 = \frac{\sum_{i=1}^{n} \phi_i^* \phi_i R_{ii}}{\left(\sum_{i=1}^{n} \phi_i^* \phi_i + \alpha^2 \phi_{L_m}^* \phi_{L_m} \right)^2}, \tag{85}$$

then we have

$$R_{ee}^R = \left(1 - \phi_0\right)^2 R_{ff} + \phi_e^2 \tag{86}$$

obviously the R_{ee}^R is a function of the parameter α and the power spectral density function ϕ_{L_m}.

5. Smoothing

In practice there are always some kinds of smoothing being used in the numerical computations. For instance, the use of the mean values of the data is a smoothing. A smoothing procedure can be used for solving the improperly posed problem. If we know the frequency composition of the function f and of the measurement error, we can design a smoothing operator (filter) to filter out the effect of errors.

Here we introduce one smoothing operator which has the spectrum

$$\phi_s = \frac{1}{1 + \alpha\omega^{\lambda}}, \quad \alpha \geq 0, \ \lambda \geq 0 \tag{87}$$

where ϕ_s is the spectrum of the smoothing operator S, and α, λ are parameters which can be chosen; $\omega = (u^2 + v^2)^{1/2}$, u, v, are frequency variables. ϕ_s is a low-pass filter because it filters out the high frequencies and lets the low frequencies pass through.

For the improperly posed problem we have the solution

$$f_s = S \cdot A^{-1} g \tag{88}$$

In the spectral domain eq. (88) can be written as

$$\omega_{f_s} = \phi_s \phi_A^{-1} \omega_g \tag{89}$$

The smoothing procedure can also be applied to the heterogeneous data. If the data are errorless, the best estimation operator H_i was given by eq. (53) and the spectrum of the solution is

$$\omega_f = \frac{\sum_{i=1}^{n} \phi_i^*}{\sum_{i=1}^{n} \phi_i \phi_i^*} \omega_{g_i} \tag{90}$$

In reality the errors are always included in the data. Except for the systematic error the measurement error are often modeled by random error and such error effects mostly the high and very high frequencies of the data. Therefore a low-pass filter can be used to decrease such effect. Another reason of the use of the low-pass filter is that the high frequencies (nearby Nyquist frequency) must be minimized in the numerical computation. Because such frequencies are mostly distorted by the measurement error, sampling error, truncation error, etc.

After the smoothing of eq. (90) we obtain a solution:

$$\omega_{f_s} = \phi_s \omega_f = \phi_s \frac{\sum_{i=1}^{n} \phi_i^* \omega_{g_i}}{\sum_{i=1}^{n} \phi_i \phi_i^*} \tag{91}$$

If the smoothing procedure is chosen properly, the effect of the errors can also be minimized and a smooth solution can be obtained from an improperly posed problem.

The smoothing error is given by

$$e^s = f - f_s \tag{92}$$

and the error covariance is

$$\begin{aligned} C_{ee}^s &= M\left\{e^s(P)\, e^s(Q)\right\} \\ &= C_{ff} - C_{ff_s} - C_{f_s f} + C_{f_s f} \end{aligned} \tag{93}$$

By using eqs. (10), (11), (88) and (92) we get the power spectral density function of the smoothing error:

$$R_{ee}^s(u, v) = \left(1 - \phi_s\right)^2 R_{ff} + \left|\phi_s \phi_A^{-1}\right|^2 R_{nn} \tag{94}$$

For the heterogeneous data the estimation error e^s is given by

$$R_{ee}^{s}(u, v) = \left(1 - \phi_s\right)^2 R_{ff} + \left| \phi_s \frac{\sum_{i=1}^{n} \phi_i^* R_{ii}}{\sum_{i=1}^{n} \phi_i^* \phi_i} \right|^2 \tag{95}$$

where R_{ii} is the power spectral density function of the measurement error ε_i.

6. Relationship Between the Least Square Collocation, Regularization and Smoothing

The relationship between the least squares collocation and the regularization method was shown in (Rummel, et al., 1979). Both of the methods are identical under some restrictions. Basically, three methods are the same and have the same property: they filter out the high frequencies in the solutions and make the solution stable and smooth. We will show that they are identical if they satisfy a few conditions.

The easiest way to show the relationship between the three methods is to inspect them in the spectral domain. We consider only the homogeneous data case. Comparing eq. (32) with (69), we find that ϕ_{H_0} and ϕ_H become identical, if the following equation holds

$$\alpha^2 \phi^*_{L_m} \phi_{L_m} = R_{nn}/R_{ff} \tag{96}$$

Rewrite eq. (69) in the form

$$\phi_{H_0} = \phi_A^{-1} \left(1 + \alpha^2 \phi^*_{L_m} \phi_{L_m} / \phi^*_A \phi_A \right)^{-1} \tag{97}$$

and compare (97) with (89) and using eq. (87), we get the equation:

$$\alpha^2 \phi^*_{L_m} \phi_{L_m} \left(\phi^*_A \phi_A \right)^{-1} = \alpha_s \omega^{\lambda} \tag{98}$$

If the regularization parameter α and the spectrum of the operator L_m satisfy eq. (97), then the regularization method is identical with the smoothing method which has a spectrum similar to eq. (87).

Putting eqs. (96) and (98) together, we get the identical condition of three methods:

$$\alpha^2 \phi^*_{L_m} \phi_{L_m} = R_{nn} R_{ff}^{-1} = \phi^*_A \phi_A \alpha_s \omega^{\lambda} \tag{99}$$

If the regularization parameter α, smoothing parameters α_s, λ and the regularization operator ϕ_{L_m} satisfy eq. (99), then the three methods are identical.

The study has shown the relationship between the three methods. They pose the same property - reducing or filtering out the high frequencies in the solution. But they are different procedures. They are identical only when all of them fulfill the condition (99).

For the regularization and smoothing method we can choose the parameters and the regularization operator L_m or different smoothing operator to get smooth solutions. Therefore they are more flexible than least squares collocation for the solving of improperly posed problems.

7. Numerical Test

In this section we take numerical tests. The goal of this numerical simulation is: To have an idea about the use of the Taylor series to get the gravity disturbance on the earth's surface by processing the aerial gravity-gradient data. The formulas above derived are used to determine the derivatives of the disturbing potential, such as T_z, T_{zz}, T_{zzz} at the mean level. We want to know how good the methods are and have a view about the magnitude of the terms, such as $\Delta h\, T_{zz}$, $1/2(\Delta h)^2 T_{zzz}$.

The test area that was chosen has the geographic latitude $32° \le \varphi \le 35°$ and the geographic longitude $257° \le \lambda \le 260°$. The 4 km x 4 km free-air anomaly for the United States (Rapp, et al., 1988) was used as the original data.

In the computation the point mass model was used. We assumed that there is a point mass layer embedded at a depth of 8 km below sea level (i.e. the geoid). The relationship between the point layer and the disturbing potential T is given by:

$$T(x, y, d) = - \sum_{i=1}^{N} \sum_{j=1}^{M} \frac{M_{ij}}{\left[(x - x_i)^2 + (y - y_j)^2 + d^2\right]^{1/2}} \qquad (100)$$

where M_{ij} is the product of the point mass at point (x_i, y_j) times the gravitational constant G, and d is the height of the computed point; N, M are the grid numbers of the area along x and y directions, the minus sign in eq. (100) is for convenience. The geometry of the point mass model is shown in Figure 2.

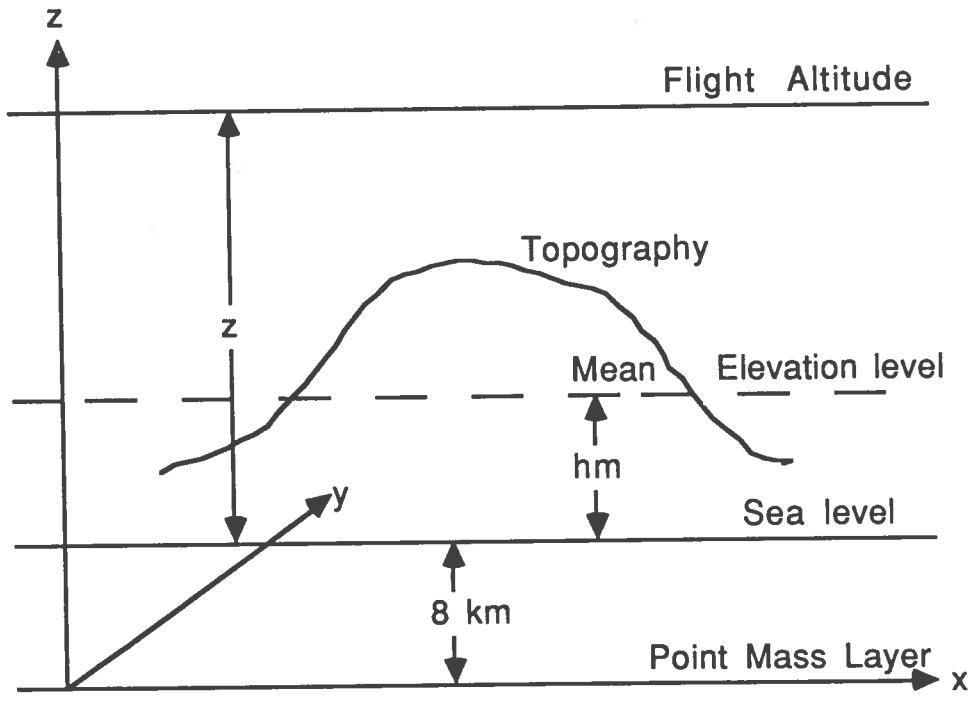

Figure 2. Geometry of the Point Mass Model (z_0 = 4 km, hm = 1.5 km)

The computational process is described generally as follows:

1. Read the free-air anomaly from the 4 km x 4 km data file (Rapp, et al., 1988) and assume the data are given on the sea level. Furthermore, the free-air anomaly is assumed to be the gravity disturbance T_z, and the formula (102) given in paragraph 7.3 is used to get the M_{ij}. d was chosen as 8 km;

2. computing T_{ij}, i, j = 1, 2, 3 on the flight level by using formulas (103), (104), (105), (107), (108), and (110) given in paragraph 7.2;

3. corrupting T_{ij} by adding random errors with error variances σ^2 = 1, 4, 25 Eötvös^2 and mean value equal zero;

4. processing the simulated gradient data to get T_i, T_{iz}, T_{izz} on the mean elevation level;

5. comparing the computed $\hat{T}_i$, $\hat{T}_{iz}$, $\hat{T}_{izz}$ with the "true" value which were computed directly from the point mass model.

In the following we give the description of the data, the formulas used and some considerations about the numerical computations.

7.1 Data Used

The gravity anomaly in 4 km x 4 km grid point values for the United States was used. In order to get higher frequencies in the solution, the data was interpolated in 2 km x 2 km grid interval by using the bicubic spline function. All computations were based on the data in 2 km x 2 km grid values. The use of 2 km x 2 km grid interval is based on the following considerations.

1. Using a small grid interval can decrease the aliasing effect in the Fourier transformation, even though we do not get more information by interpolating the 4 km x 4 km gravity anomaly into 2 km x 2 km grid point values;

2. The evaluation of the formulas, such as given in the next paragraph, can be more accurate by using 2 km x 2 km grid than using 4 km x 4 km grid. Using the smaller grid can increase the computation accuracy (cf. Tziavos, et al., 1988).

The statistics of gravity anomaly Δg in this area is given in Table 1.

Table 1. Statistics of the Gravity Anomaly Δg in the Test Area.
(mgal)

mean value	RMS value	maximum	minimum
-8.82	24.48	78.21	-76.17

The contour map of the gravity anomaly in the test area is shown in Figure 3.

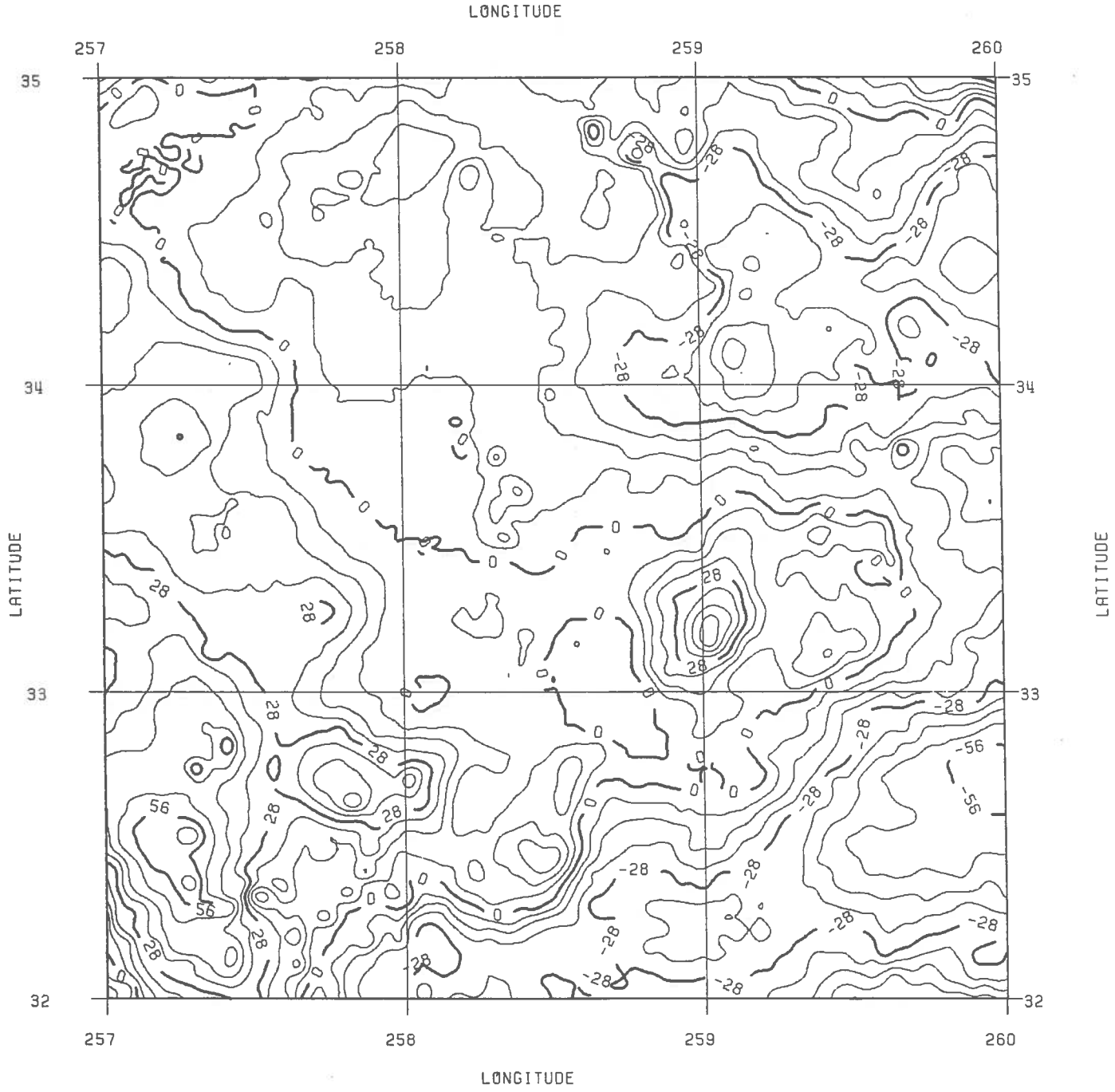

Figure 3. Contour Map of the Gravity Anomaly in Test Area.
Contour Interval = 7 mgal

7.2 Formulas Used

Before the numerical tests were taken, the formulas which would be used are written in the following. The spectra of the differential operators used occur in the airborne gravity gradiometry are given in Table 2 (cf. Vassiliou, 1986). The definition of the spectra of the operators are given in eq. (22).

Table 2. Spectra of the Differential Operators

Operators	Spectra
$\frac{\partial}{\partial x}$	$j\,2\pi u$
$\frac{\partial}{\partial y}$	$j\,2\pi v$
$\frac{\partial}{\partial z}$	$-2\pi\omega$
$\frac{\partial^n}{\partial x^k \partial y^l \partial z^p}$	$(j\,2\pi u)^k (j\,2\pi v)^l (-2\pi\omega)^p$

Here we have $k + l + p = n$; $k, l, p = 0, 1, 2, \ldots$

It is easy to find the spectrum of the upward continuation operator U defined by eq. (1):

$$\phi_U = e^{-2\pi\omega Z_H} \tag{101}$$

The relationship between the disturbing potential T and the mass point M_{ij} is given by eq. (100). The derivatives of the disturbing potential T_i, T_{ij}, $i, j = 1, 2, 3$ can be derived from eq. (100) (cf. Vassiliou, 1986):

$$T_z = \sum_{i=1}^{M} \sum_{j=1}^{N} \frac{d}{l^{3/2}} M_{ij} \tag{102}$$

$$T_{zz} = \sum_{i=1}^{M} \sum_{j=1}^{N} \frac{(x-x_i)^2 + (y-y_j)^2 - 2d^2}{l^{5/2}} M_{ij} \tag{103}$$

$$T_{zx} = -\sum_{i=1}^{M} \sum_{j=1}^{N} \frac{3(x-x_i)\,d}{l^{5/2}} M_{ij} \tag{104}$$

$$T_{zy} = -\sum_{i=1}^{M}\sum_{j=1}^{N} \frac{3(y-y_j)\,d}{l^{5/2}} M_{ij} \tag{105}$$

$$T_{x} = \sum_{i=1}^{M}\sum_{j=1}^{N} \frac{x-x_i}{l^{3/2}} M_{ij} \tag{106}$$

$$T_{xx} = \sum_{i=1}^{M}\sum_{j=1}^{N} \frac{(y-y_j)^2 + d^2 - 2(x-x_i)^2}{l^{5/2}} M_{ij} \tag{107}$$

$$T_{xy} = -\sum_{i=1}^{M}\sum_{j=1}^{N} \frac{3(x-x_i)(y-y_j)}{l^{5/2}} M_{ij} \tag{108}$$

$$T_{y} = \sum_{i=1}^{M}\sum_{j=1}^{N} \frac{y-y_j}{l^{3/2}} M_{ij} \tag{109}$$

$$T_{yy} = \sum_{i=1}^{M}\sum_{j=1}^{N} \frac{(x-x_i)^2 + d^2 - 2(y-y_j)^2}{l^{5/2}} M_{ij} \tag{110}$$

where $l = [(x-x_i)^2 + (y-y_j)^2 + d^2]^{1/2}$.

Taking the Fourier transformation of the formulas (102) - (110), and using Table 2, we have:

$$F\{T\} = F\{M_{ij}\}\left(-\frac{1}{\omega} e^{-2\pi\omega d}\right) \tag{111}$$

$$F\{T_z\} = F\{M_{ij}\}\left(2\pi\, e^{-2\pi\omega d}\right) \tag{112}$$

$$F\{T_{zz}\} = F\{M_{ij}\}\left\{-(2\pi)^2\, \omega e^{-2\pi\omega d}\right\} \tag{113}$$

$$F\{T_{zx}\} = F\{M_{ij}\}\left\{j(2\pi)^2\, u e^{-2\pi\omega d}\right\} \tag{114}$$

$$F\{T_{zy}\} = F\{M_{ij}\}\left\{j(2\pi)^2\, v e^{-2\pi\omega d}\right\} \tag{115}$$

$$F\{T_{x}\} = F\{M_{ij}\}\left\{-j\frac{2\pi u}{\omega} e^{-2\pi\omega d}\right\} \tag{116}$$

$$F\{T_{xx}\} = F\{M_{ij}\}\left\{\frac{(2\pi u)^2}{\omega} e^{-2\pi\omega d}\right\} \tag{117}$$

$$F\{T_{xy}\} = F\{M_{ij}\}\left\{\frac{(2\pi)^2}{\omega} uve^{-2\pi\omega d}\right\} \tag{118}$$

$$F\{T_y\} = F\{M_{ij}\}\left\{-j\frac{2\pi v}{\omega} e^{-2\pi\omega d}\right\} \tag{119}$$

$$F\{T_{yy}\} = F\{M_{ij}\}\left\{\frac{(2\pi v)^2}{\omega} e^{-2\pi\omega d}\right\} \tag{120}$$

Here we should not confuse the subscript j with the imaginary number $j = \sqrt{-1}$.

In the numerical computations eqs. (111) - (120) were discretizated and were evaluated by using the fast Fourier transformation (FFT). The first and second derivatives of the disturbing potential were computed at the flight level and mean elevation level by using eqs. (111) - (120).

After the computations of the second derivatives of the disturbing potential T_{ij} at the flight level, the normal distribution of the random noise with the variance $\sigma^2 = 1, 4, 25$ Eötvös^2 was added to the computed T_{ij}. In processing the corrupted data to determine the derivatives of the disturbing potential T_i, T_{iz}, T_{izz} on the mean elevation level, the regularization method was used.

It was assumed that the disturbing potential T and its partial derivatives to z up to third order are smooth at the mean elevation level. For the word "smooth" we understand it under such meaning: The disturbing potential T has continuous partial derivatives up to third order. In fact, the disturbing potential T has continuous partial derivatives up to all orders above the earth's surface. Because the analytical downward continuation is used, we constrained the disturbing potential has continuous partial derivatives up to 3rd order above the mean elevation level. We took the regularization operator in eq. (75) as

$$L_m = U\frac{\partial^3}{\partial z^3} \tag{121}$$

where U is the upward continuation operator.

The spectrum of the operator L_m is given by

$$\phi_{L_m} = -(2\pi\omega)^3 \phi_U, \tag{122}$$

Six components of the second derivatives were used to determine T_i, i = 1, 2, 3 on the mean elevation level. The observation equations are

$$\underline{l} = \underline{A}_x T_x + \underline{\varepsilon}_x \tag{123}$$

$$\underline{l} = \underline{A}_y T_y + \underline{\varepsilon}_y \tag{124}$$

$$\underline{l} = \underline{A}_z T_z + \underline{\varepsilon}_z \tag{125}$$

where $\underline{l}$ is the observation vector which has the components l_i, i = 1, 2, ... 6, the measured second derivatives of the disturbing potential; $\underline{A}_x$, $\underline{A}_y$ and $\underline{A}_z$ are vector operators; $\underline{\varepsilon}$ is the vector of the measurement error. As a specific example eq. (123) is written in the form:

$$\begin{bmatrix} T^1_{xz} \\ T^1_{yz} \\ T^1_{zz} \\ T^1_{xx} \\ T^1_{xy} \\ T^1_{yy} \end{bmatrix} = \begin{bmatrix} A_1 \\ A_2 \\ A_3 \\ A_4 \\ A_5 \\ A_6 \end{bmatrix} T_x + \begin{bmatrix} \varepsilon_1 \\ \varepsilon_2 \\ \varepsilon_3 \\ \varepsilon_4 \\ \varepsilon_5 \\ \varepsilon_6 \end{bmatrix} \tag{123'}$$

where T^1_{xz}, T^1_{yz}, ... are the measured gradients of the gravity disturbance; ε_1, ε_2,... are the corresponding measurement error.

The best estimates of the T_x, T_y and T_z in eq. (123), (124) and (125) are given by:

$$\hat{T}_x(x, y, h_m) = F^{-1}\left\{k(u, v)\, j\, 2\pi u\right\} \tag{126}$$

$$\hat{T}_y(x, y, h_m) = F^{-1}\left\{k(u, v)\, j\, 2\pi v\right\} \tag{127}$$

$$\hat{T}_z(x, y, h_m) = F^{-1}\left\{k(u, v)(-2\pi\omega)\right\} \tag{128}$$

where the symbol " ^" denotes the estimate of the function, and k (u, v) is given by:

$$k(u,v)=\frac{\phi_U^{-1}\sum_{i=1}^{6}\phi_i^{*}\,\omega_{g_i}}{\sum_{i=1}^{6}\phi_i^{*}\,\phi_i+\alpha^2(2\pi\omega)^6} \tag{129}$$

Here we have used eqs. (81) and (122). The ω_{gi} is the Fourier transform of the observations T_{ij}. From eq. (126) - (128) one can see that the k (u, v) is nothing but the spectrum of the disturbing potential T determined by using the gradient data T_{ij}. If the T_{ij} is ordered as in (123'), then we have:

$$\phi_1=-j(2\pi)^2 u\omega\,,\quad \phi_2=-j(2\pi)^2 v\omega\,,$$

$$\phi_3=(2\pi)^2\omega^2\,,\quad \phi_4=-(2\pi)^2 u^2\,,$$

$$\phi_5=-(2\pi)^2 uv\,,\quad \phi_6=-(2\pi)^2 v^2\,. \tag{130}$$

Insert (130) into (129), we get

$$k(u,v)=\frac{\phi_U^{-1}\sum_{i=1}^{6}\phi_i^{*}\,\omega_{g_i}}{\left(3\omega^4-u^2v^2\right)+\alpha^2(2\pi\omega)^6} \tag{131}$$

In the numerical computations the regularization parameter α has taken the value 0.07.

In the same manner we have the formulas for the second and third derivatives on the mean elevation level:

$$\hat{T}_{xz}(x,y,h_m)=F^{-1}\left\{k(u,v)(2\pi)^2(-ju\omega)\right\} \tag{132}$$

$$\hat{T}_{yz}(x,y,h_m)=F^{-1}\left\{k(u,v)(2\pi)^2(-jv\omega)\right\} \tag{133}$$

$$\hat{T}_{zz}(x,y,h_m)=F^{-1}\left\{k(u,v)(2\pi)^2\omega^2\right\} \tag{134}$$

and

$$\hat{T}_{xzz}(x,y,h_m)=F^{-1}\left\{k(u,v)(2\pi)^3(ju\omega^2)\right\} \tag{135}$$

$$\hat{T}_{yzz}(x, y, h_m) = F^{-1}\left\{k(u, v)(2\pi)^3\left(jv\omega^2\right)\right\} \tag{136}$$

$$\hat{T}_{zzz}(x, y, h_m) = F^{-1}\left\{k(u, v)(2\pi)^3\left(-\omega^3\right)\right\} \tag{137}$$

The formulas (126) - (137) were discretizated and evaluated by using the fast Fourier transformation.

If we use the smoothing method, according to the equation (98), the parameter α_s, λ are chosen

$$\alpha_s = \frac{1}{3}\alpha^2 = 100, \quad \lambda = 2 \tag{138}$$

The spectrum of the smoothing operator is

$$\phi_s = \frac{1}{1 + \alpha_s \omega^2} = \frac{1}{1 + 100\,\omega^2} \tag{139}$$

The least squares collocation method can also be used. But the power spectral density function of the disturbing potential and of the measurement error have to be properly chosen.

The regularization error was not computed by using the formulas like (86), because the "true" value could be computed directly. The difference between the "true" values and the computed values were computed and the results are shown in the following section.

If we have no "true" values, as it should be in practice we can choose the spectral density function of the disturbing potential T and of the error ε, the estimation error (regularization error, smoothing error) can be estimated by using the above derived formulas.

7.3 Considerations of the Singularity and Recovery of the Spectra of the Gravity Disturbance From Gradient Data

In the above derived formulas we have the singularity problem. The formulas, e.g. eq. (131), are not defined at the origin. Such a problem can be catalogued by the singular integral problem. A theoretical study of singular integrals and integral equations is given in Miklin (1965). The study of the singular integrals in the physical geodesy can be found in (Sünkel, 1977; Wang, 1986).

Here we consider the singularity problem in the spectra domain. As a common example, we consider the Stokes' integral. In the planar approximation we have:

$$N = \frac{1}{2\pi\gamma}\int\!\!\int_{-\infty}^{\infty} \frac{\Delta g}{l}\, dx\, dy \tag{140}$$

where N is the geoid undulation, γ, and Δg are the normal gravity and gravity anomaly, respectively. Applying the Fourier transformation to eq. (140) we get

$$\omega_N = \frac{1}{2\pi\gamma\omega}\omega_g \tag{141}$$

where ω_N, ω_g are the Fourier transformation of the geoid undulation and the gravity anomaly, respectively.

We have two methods to compute eq. (140). One is taking the discrete Fourier transformation to eq. (140). The kernel l^{-1} has a singularity at the point (x = 0, y = 0). The treatment of the singularity can be found in (Heiskanen and Moritz, p. 121; Schwarz, et al., 1989).

Eq. (141) can also be used to compute the geoid undulation. The only question is, what kind of value eq. (141) should be taken at the point (u = 0, v = 0)? It will be shown that the choice of the value ω_N (0, 0) effects on the geoid a constant bias.

Let

$$\omega_N(0,0) = \beta\,\omega_g(0,0) \neq 0 \tag{142}$$

where β is an arbitrary constant. Notice that

$$\omega_g(0,0) = \int\int_{-\infty}^{\infty} e^{2\pi j\,(0.x+0.y)}\,\Delta g\,(x,y)\,dx\,dy$$

$$= \int\int_{-\infty}^{\infty} \Delta g\,(x,y)\,dx\,dy \tag{143}$$

If the integral in eq. (143) is limited in a local area, as the case in practice, ω_g (0, 0) is not always equal to zero. Assume that eq. (141) is discretized and inversed by using the discrete Fourier transformation, then the ω_N (0, 0) has the contribution to the geoid.

$$\delta N = \frac{1}{MN}\sum_{m=0}^{M}\sum_{n=0}^{N}\beta\,\omega_g(0,0)\,e^{-2\pi j\left(\frac{m\,0}{M}+\frac{n\,0}{N}\right)}$$

$$= \beta\,\omega_g(0,0) \tag{144}$$

where δN is the change of the geoid due to the different choices of the ω_N (0, 0). δN is a constant everywhere. If we set ω_g (0, 0) = 0, then δN = 0. Therefore the geoid undulation from eq. (141) may have a constant difference with the geoid undulation direct from the Stoke's integral (140). In order to remove this bias, other data, such as reference fields, should be used.

Another question is: Can we recover all spectra of the gravity disturbance from the gradient data? The answer is no. For example, the relationship between T_z and T_{zx} is

$$\omega_{T_{zx}} = j2u\omega_{T_z} \tag{145}$$

If we want to recover ω_{T_z} from $\omega_{T_{zx}}$, we have

$$\omega_{T_z} = -j\frac{1}{2\pi u}\omega_{T_{zx}} \tag{146}$$

At the line u = 0, the spectra ω_{T_z} are not defined. A common way in the numerical computation is to set

$$\omega_{T_z}(0, v) = 0, \qquad v \in (-\infty, +\infty). \tag{147}$$

But in reality eq. (147) is not correct, since the spectra $\omega_{T_z}(0, v)$ should not be equal to zero. The conclusion is: The spectrum of T_z cannot be recovered from the spectra T_{zx} entirely.

In the numerical computations, we have to take the assumption (147). Therefore it is not good enough using T_{xz} (including T_{yz}) to determine T_z because we cannot recover all frequencies of T_z from T_{zx} or T_{zy}.

A better recovery of the spectrum of T_z can be achieved from T_{zz}:

$$\omega_{T_z} = -\frac{1}{2\pi\omega}\omega_{T_{zz}} \tag{148}$$

This function is not defined at the origin (0, 0). If we assume the mean value T_z is equal to zero, based on eq. (143) we have:

$$\omega_{T_z}(0, 0) = 0 \tag{149}$$

and we can get all frequencies of T_z from T_{zz}. If the ω_{T_z} is not equal to zero, we still have to take (149) in the numerical computation. But the information on the bias of T_z has to be provided by other data, such as the point disturbance component values on the ground (Jekeli, 1986).

The best way to recover the frequencies of the gravity disturbance is the use of all components of the second derivatives of the disturbing potential. From eqs. (128) and (131) we can see, frequency of T_z from all data is not defined only at the point (0, 0). We define the frequency of T_z at this point as equal to zero, and the frequency $\omega_{T_z}(0, 0)$ is obtained from tie point disturbance component values or another data.

Summary: We can recover all frequencies of the gravity disturbance by processing the aerial gravity-gradient data except the mean value. The mean value of the gravity disturbance must be provided by tie point values or another data.

7.4 Results

In the preceeding sections we described the data, the formulas used. In this section we give the computational results. The derivatives of the disturbing potential were determined on the mean elevation level and compared with the "true" values which were computed from the point mass model directly.

In Table 3 we give the statistics of the differences (errors) between the computed and the "true" values for the partial derivatives of the disturbing potential to z. In the numerical computation eqs. (128), (134) and (137) were used. The regularization function was chosen as described in section 7.2.

Table 3. Statistics of the Differences Between the Computed and the "True" Values

	Noise level (E)	mean	RMS	max	min
T_z (mgal)	$\sigma = 1$	- 0.29	0.52	2.57	- 3.72
	$\sigma = 2$	- 0.29	0.60	2.78	- 3.94
	$\sigma = 5$	- 0.29	0.99	3.67	- 4.76
T_{zz} (mgal/km)	$\sigma = 1$	- 0.03	0.26	1.47	- 1.64
	$\sigma = 2$	- 0.03	0.47	2.13	- 1.95
	$\sigma = 5$	- 0.03	1.14	4.35	- 4.73
T_{zzz} (mgal/km^2)	$\sigma = 1$	$- 0.84 \times 10^{-3}$	0.40	1.71	- 1.69
	$\sigma = 2$	$- 0.87 \times 10^{-3}$	0.77	3.05	- 1.95
	$\sigma = 5$	$- 0.96 \times 10^{-3}$	1.90	7.78	- 6.97

From Table 3 we can see that the random noises have no significant effects on T_z. In the computations the regularization was used and the effects of the noise have been mostly removed. This is not the same as expected (Jekeli, 1987). The reasons may be:

1. We used the gravity anomaly in a not very rough (gravity anomaly wise) area. The spectra of Δg consisted mostly by lower frequencies. The power spectral density function of the data is shown in Figure 4. The amplitude of the high frequencies of the data is small and should have no significant contribution to T_z, T_{zz} and T_{zzz}. The high frequencies of the measurement noise and the high frequencies of the data were filtered out and the results were not changed significantly from the "true" value.

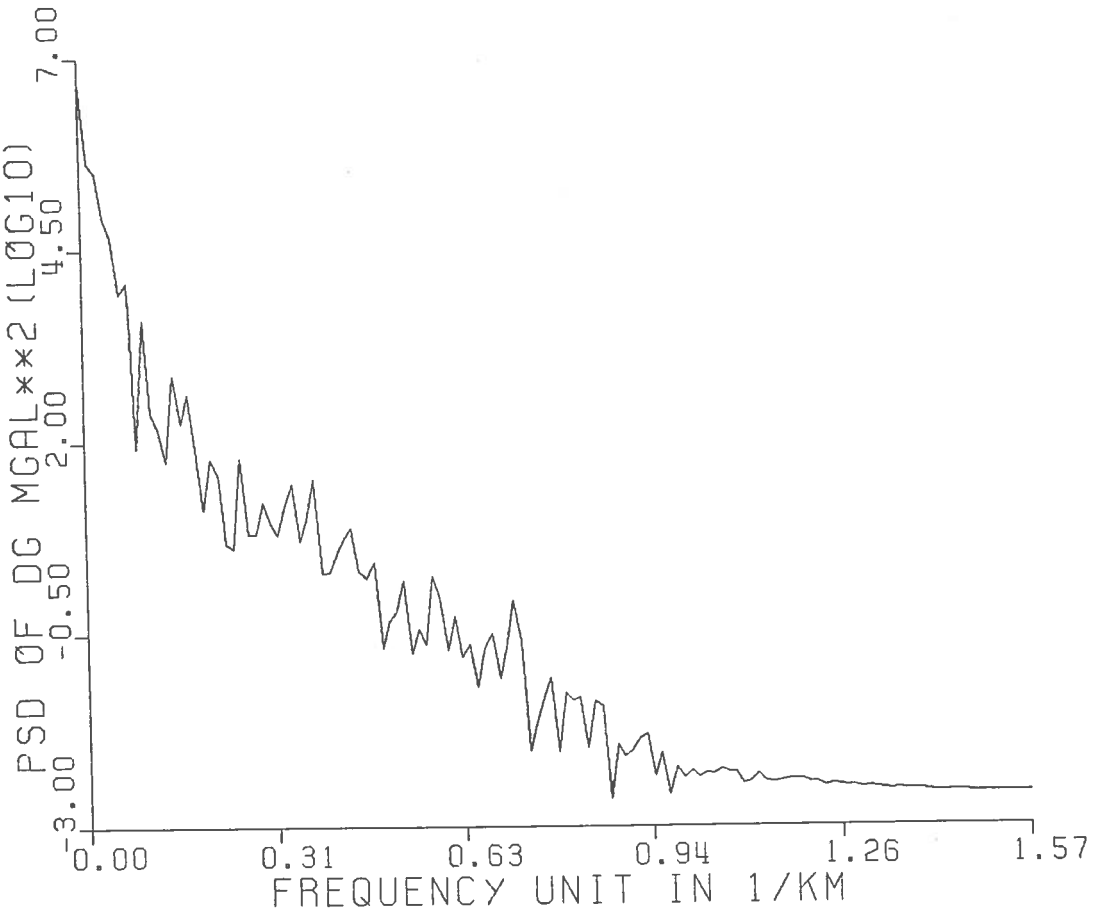

Figure 4. Power Spectral Density of the Gravity Anomaly Δg in Test Area

2. An important thing in the numerical simulation is the choice of the grid inteval. The gradient data used were regularly distributed in a 2 km x 2 km grid interval. The small grid interval minimized the aliasing effect. A study about the computation accuracy with the grid spacing, flight altitude can be found in (Tziavos, et al., 1988). Even though where they were talking about the computation of the topographic effect on the gradient data, we get some idea about the relationship between the computation accuracy and the ratio of the grid spacing/flight altitude. In our computation the ratio of grid spacing/flight altitude was 2/2.5 and it met the computation accuracy.

3. The ratio of signal/noise is defined by the RMS value of signal/RMS value of noise. In the numerical computations this ratio was reasonable. For example, for the gradient T_{zz} we have the signal/noise ratio equal 8, when the random noise has variance $\sigma = 1$ Eötvös. A very interesting phenomenon is, even if $\sigma = 5$ Eötvös when the ratio of the signal/noise equal 1.6, the results for T_z are still good. The reason may be: the random errors pose high frequencies and they are filtered out by using the regularization method; the second reason is that all components of the gravity gradient have been used and it improved the results.

Of course we cannot expect to obtain good results of T_{zzz} by processing the aerial gradient data. The high derivatives of the disturbing potential T_{zzz} is more sensitive to the measurement error.

In the following we determine the derivatives of the disturbing potential up to third order on the mean elevation level, and the Taylor's series are used to get the gravity disturbance on the earth's surface. The difference between the "true" values and the computed values are given in the

following tables. The second correction term of eq. (9) is also included and the results are presented in the tables. The results without the second correction term of (9) are also shown in the following tables.

Table 4. Statistics of the Differences of

$$T_z - \left(\hat{T}_z + \Delta h\, \hat{T}_{zz} + \frac{1}{2}(\Delta h)^2 \hat{T}_{zzz}\right)$$

unit mgal

noise level (E)	mean	RMS	max	min
$\sigma = 1$	- 0.06	1.12	7.25	- 7.55
$\sigma = 2$	- 0.06	1.94	8.52	- 9.08
$\sigma = 5$	- 0.06	4.61	18.83	- 17.54

Table 5. Statistics of the Difference of

$$T_z - \left(\hat{T}_z + \Delta h\, \hat{T}_{zz}\right)$$

unit mgal

noise level (E)	mean	RMS	max	min
$\sigma = 1$	- 0.06	0.91	7.89	- 9.02
$\sigma = 2$	- 0.06	1.26	8.51	- 9.43
$\sigma = 5$	- 0.06	2.61	10.39	- 12.04

Comparing Table 4 with 5 we find: If the accuracy of the gravity gradient data is poor, e.g., σ = 5 E, the term 0.5 $(\Delta h)^2$ T_{zzz} is corrupted by the errors and it is not usable (compare the results in Table 4 and 5 when σ = 5 E.). But this term still gives some contributions to the big values of T_z (compare the results in Table 4 and 5 when σ = 1 E.) while the RMS values becomes bigger. It is expected that this term gives significant contributions to the big absolute values of T_z if the gradient data are accurate and in good distribution.

The map of the contour line for the estimated $\hat{T}_z$ was drawn in Figure 5. Comparing Figure 3 with 5, one can find the $\hat{T}_z$ is smoother and smaller (absolute magnitude). Figure 6 shows the contribution of the correction term $\Delta h\, \hat{T}_{zz}$, in test area. A few significant corrections are in the rough gravity anomaly area. The contribution of the correction term $1/2(\Delta h)^2\, \hat{T}_{zzz}$ is shown in Figure 7. The correction is small and rough. This correction can become very small after some kinds of smoothing, e.g., the results are averaged into mean block values. Figure 8 gives the computed T_z in the test area. In comparison with Figure 3 one can say that the recovery of the gravity disturbance by processing the gradient data are successful. Figure 9 gives the difference between the "true" values and the computed values. Although the difference (error) can reach 5-7 mgal at some points, but it can become smaller when the results are averaged into mean block values.

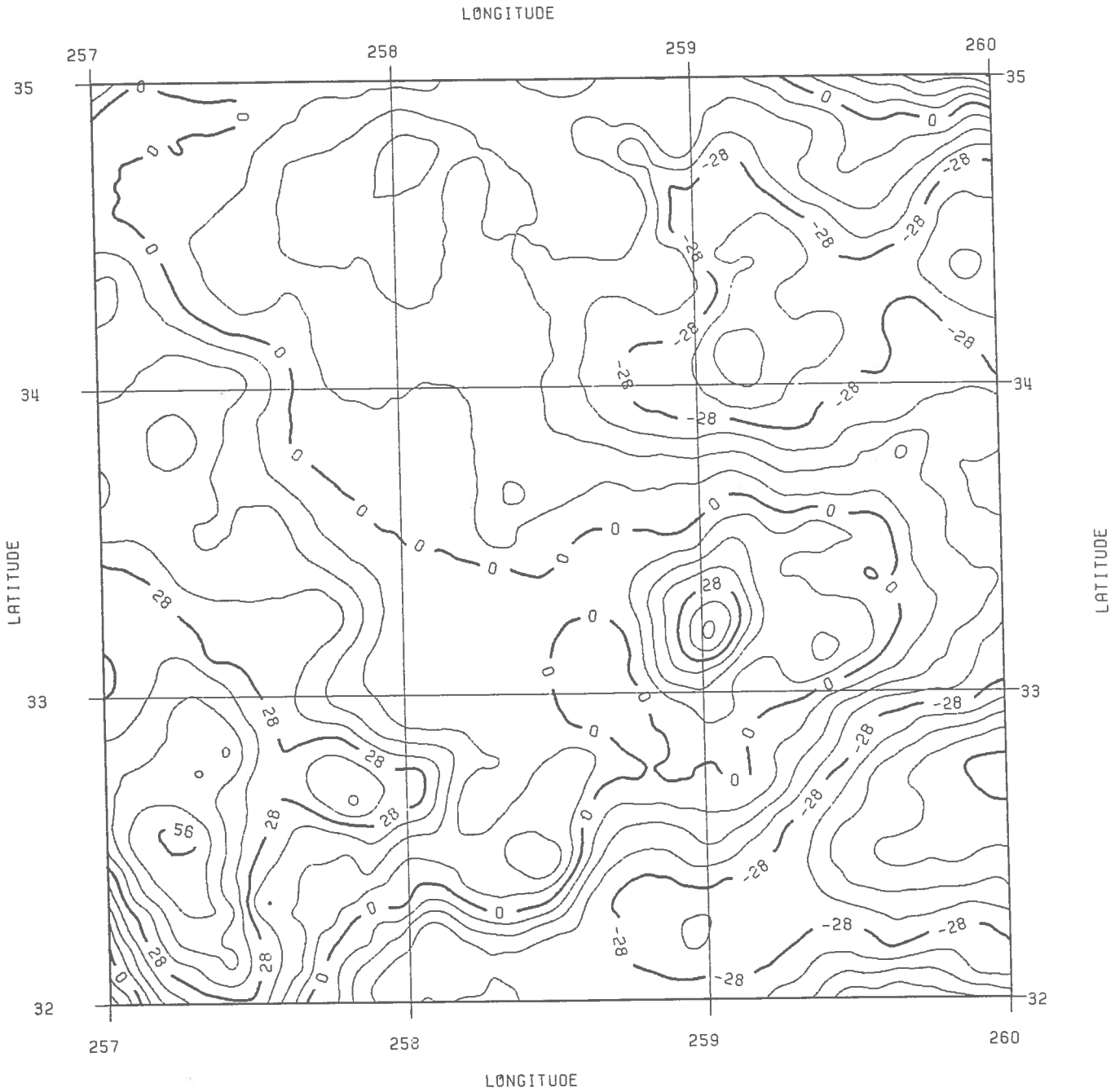

Figure 5. Contour Map of $\hat{T}_z$ in Test Area
Contour Interval = 7 mgal

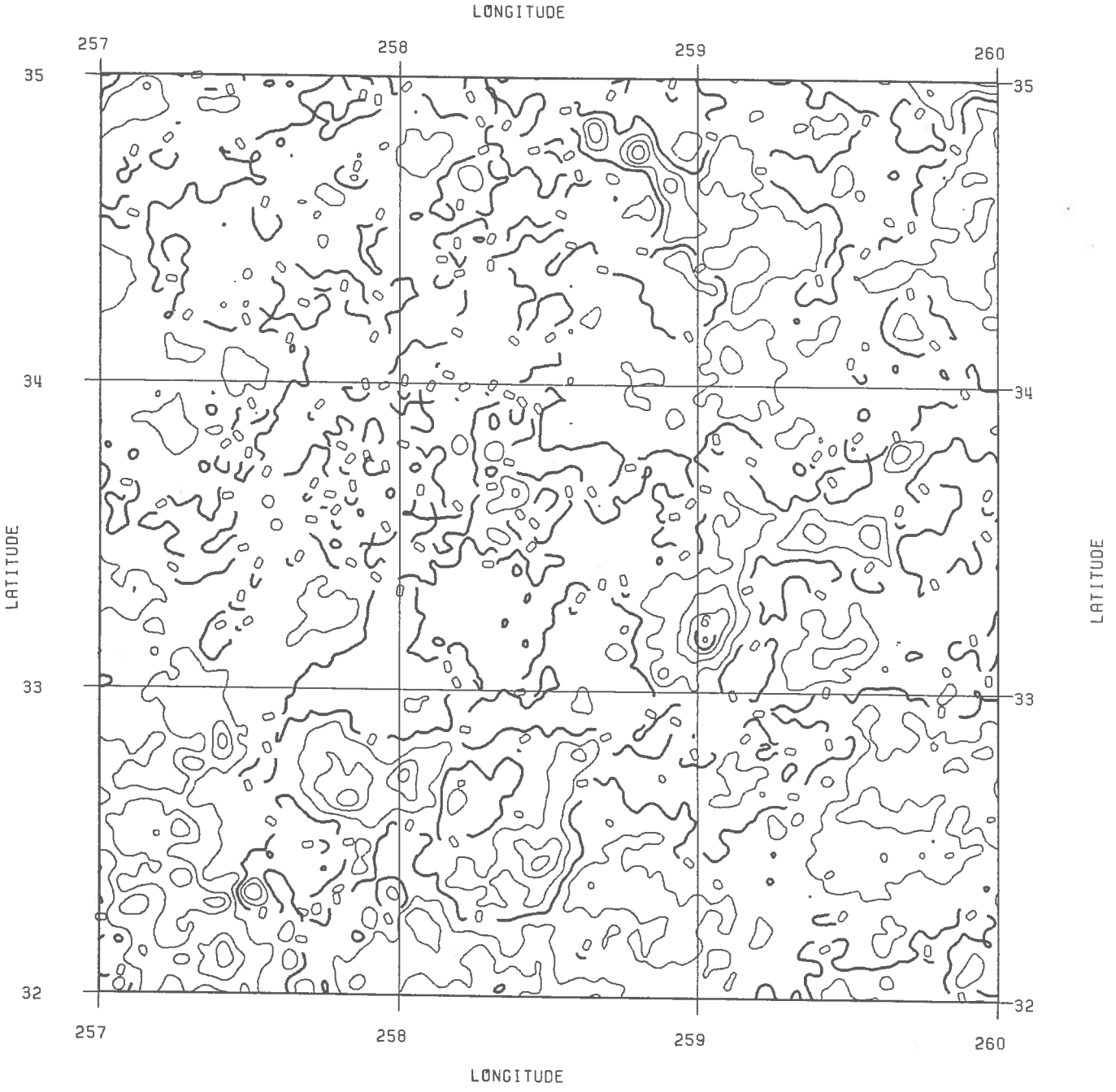

Figure 6. Contour Map of $\Delta h \cdot \hat{T}_{zz}$ in Test Area
Contour Interval = 1.5 mgal

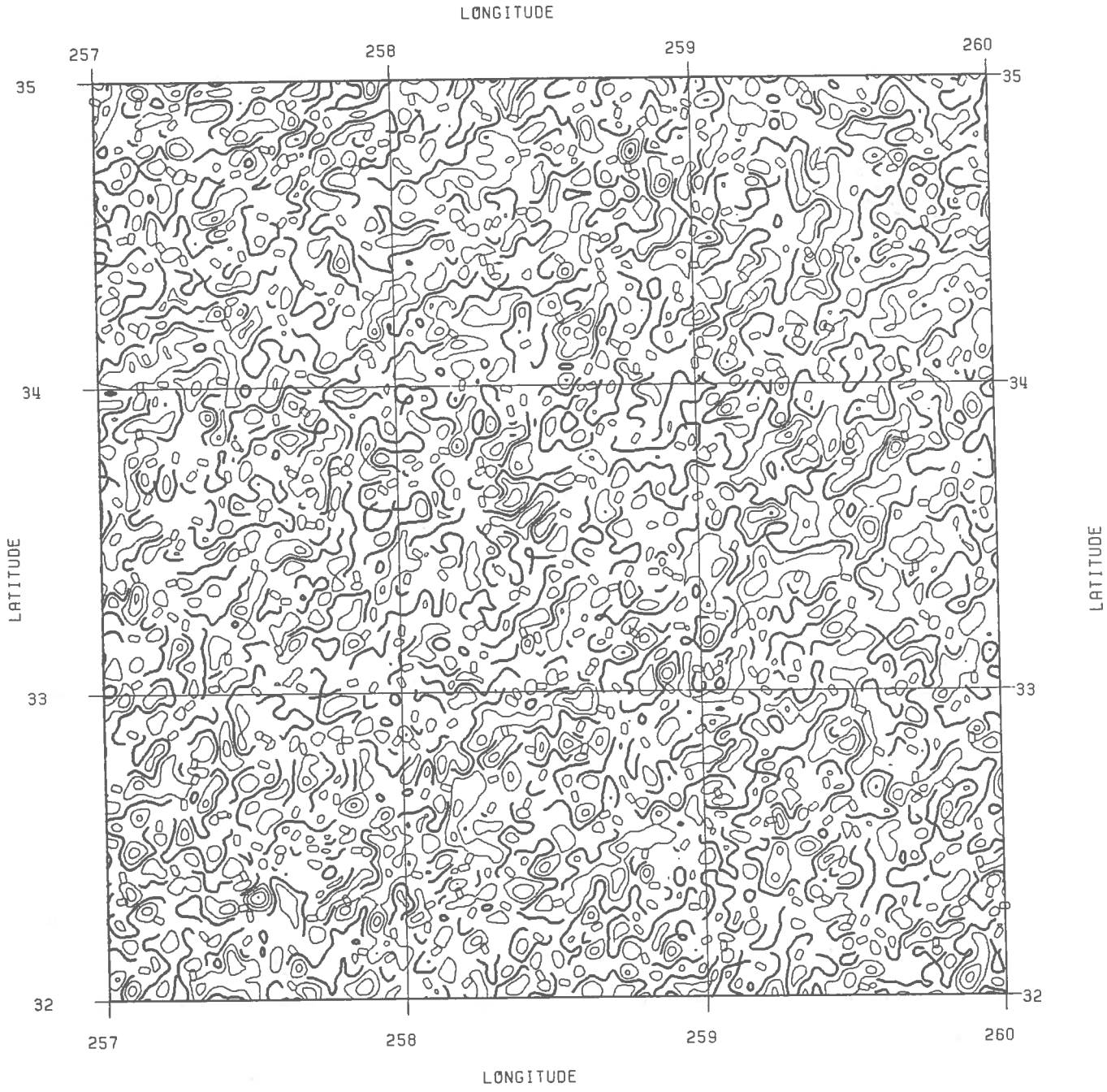

Figure 7. Contour Map of $(\Delta h)^2 \hat{T}_{zzz}$ in Test Area
Contour Interval = 0.5 mgal

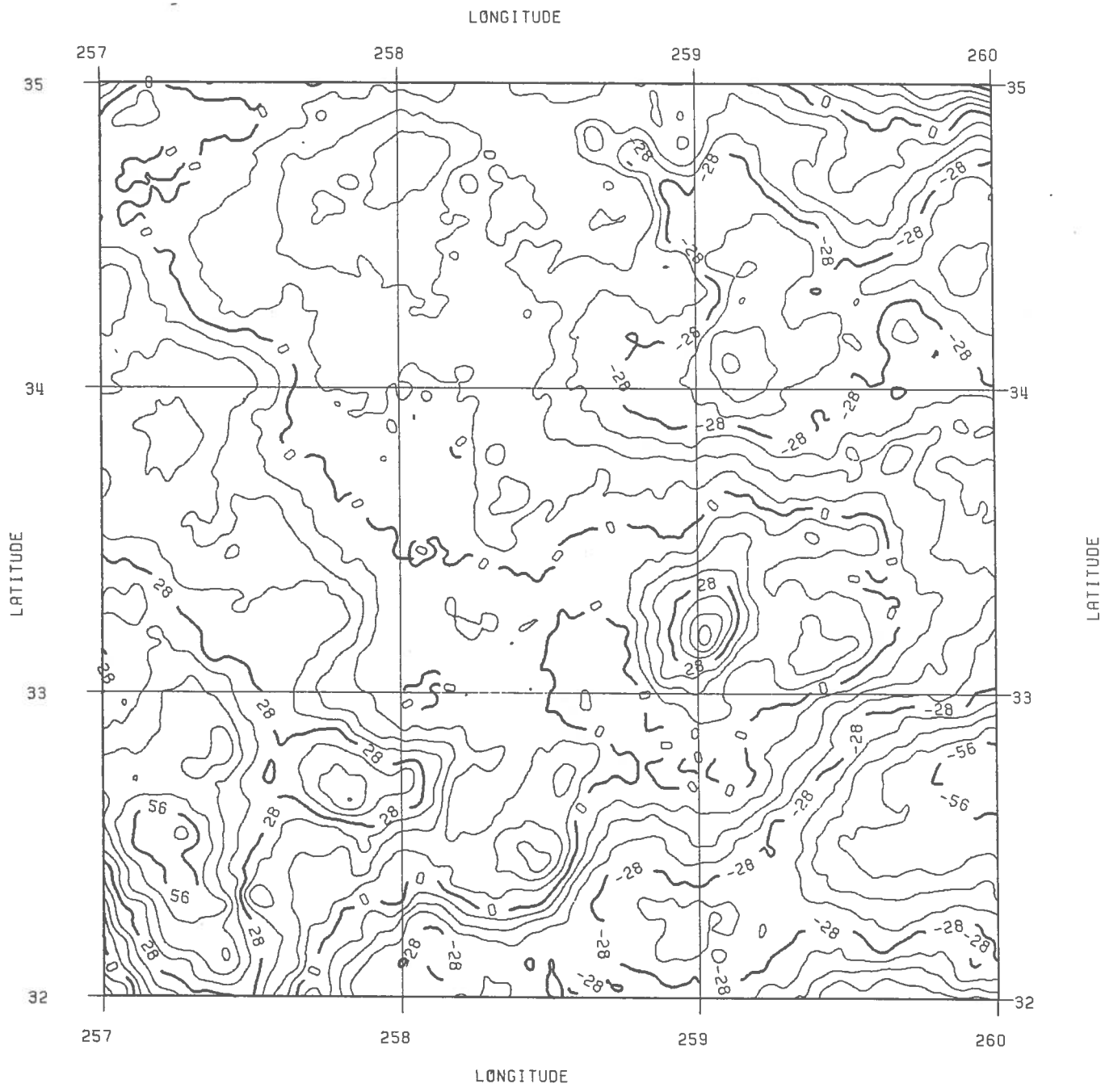

Figure 8. Contour Map of the Computed Gravity Disturbance $\hat{T}_z + \Delta h\ \hat{T}_{zz} + 1/2\ (\Delta h)^2\ \hat{T}_{zzz}$
Contour Interval = 7 mgal

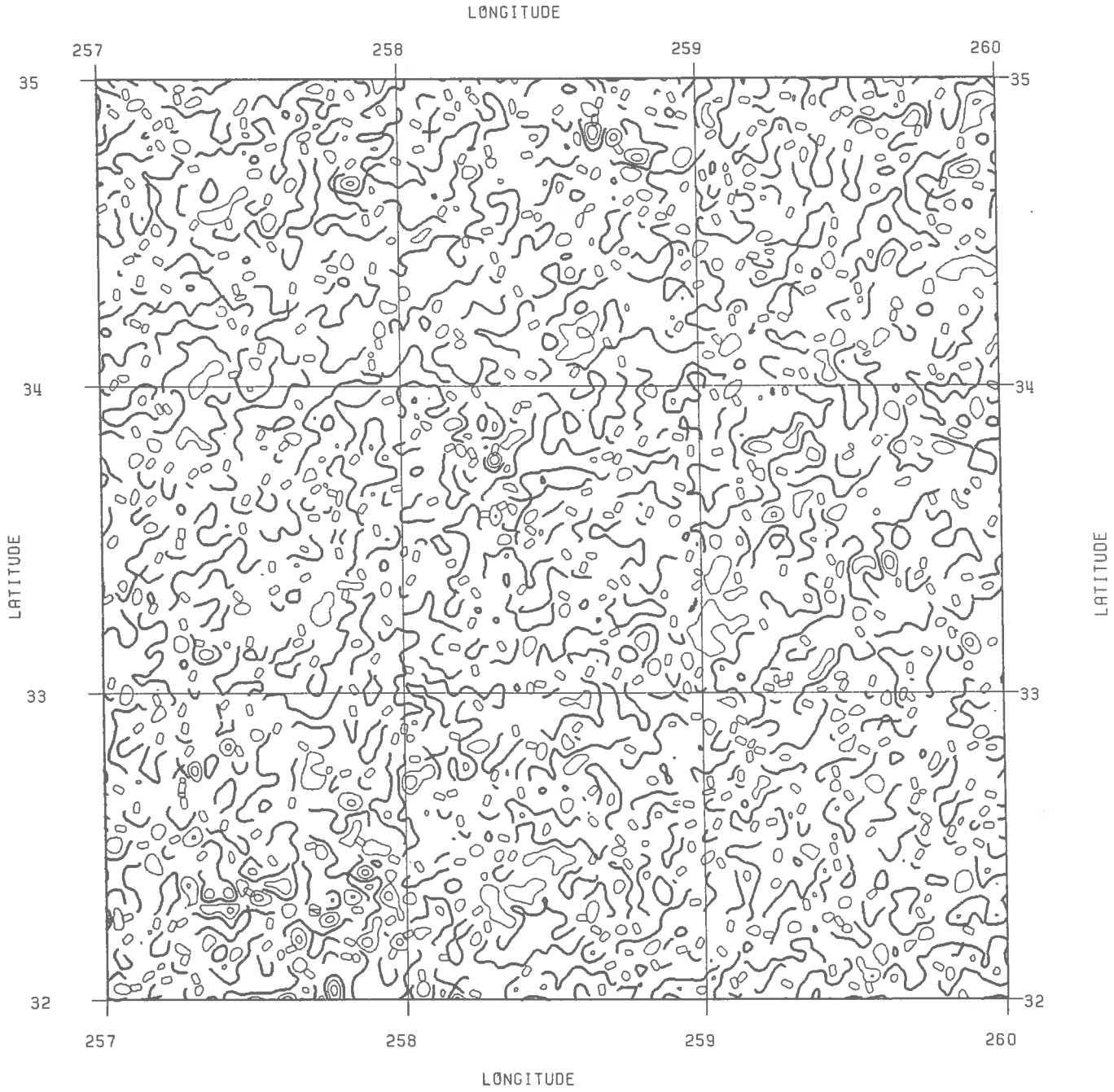

Figure 9. Contour Map of the Difference $T_z - (\hat{T}_z + \Delta h\ \hat{T}_{zz} + 1/2\ (\Delta h)^2\ \hat{T}_{zzz})$
Contour Interval = 2 mgal

Similarly, the computation at results for T_x, T_y are given in Table 6-11.

Table 6. Statistics of Differences Between the Results and the "True Value"
unit mgal

	Noise level (E)	mean	RMS	max	min
T_x (mgal)	$\sigma = 1$	0.71×10^{-2}	0.26	2.84	- 2.11
	$\sigma = 2$	0.01	0.33	2.84	- 2.18
	$\sigma = 5$	0.02	0.64	2.91	- 2.95
T_{xz} (mgal/km)	$\sigma = 1$	$- 0.35 \times 10^{-3}$	0.18	1.00	- 1.00
	$\sigma = 2$	$- 0.50 \times 10^{-3}$	0.33	1.37	- 1.34
	$\sigma = 5$	$- 0.94 \times 10^{-3}$	0.81	3.01	- 3.31
T_{xzz} (mgal/km^2)	$\sigma = 1$	$- 0.32 \times 10^{-5}$	0.28	1.19	- 1.03
	$\sigma = 2$	$- 0.44 \times 10^{-4}$	0.54	2.37	- 2.03
	$\sigma = 5$	$- 0.17 \times 10^{-3}$	1.35	5.89	- 5.05

Table 7. Statistics of Differences of

$$T_x - \left(\hat{T}_x + \Delta h \, \hat{T}_{xz} + \frac{1}{2} (\Delta h)^2 \hat{T}_{xzz} \right)$$

unit mgal

noise level (E)	mean	RMS	max	min
$\sigma = 1$	0.01	0.78	5.39	- 4.82
$\sigma = 2$	0.01	1.37	5.78	- 5.74
$\sigma = 5$	0.03	3.26	13.20	- 12.36

Table 8. Statistics of the Differences of

$$T_x - \left(\hat{T}_x + \Delta h \, \hat{T}_{zx} \right)$$

unit mgal

noise level (E)	mean	RMS	max	min
$\sigma = 1$	0.01	0.63	6.48	- 5.67
$\sigma = 2$	0.01	0.88	6.56	- 5.77
$\sigma = 5$	0.03	1.84	7.41	- 7.44

Table 9. Statistics of Differences Between the Results and the "True Value"
unit mgal

	Noise level (E)	mean	RMS	max	min
T_y (mgal)	$\sigma = 1$	0.11	0.31	1.97	- 2.89
	$\sigma = 2$	0.11	0.38	2.19	- 2.94
	$\sigma = 5$	0.12	0.67	2.85	- 3.35
T_{yz} (mgal/km)	$\sigma = 1$	-0.90×10^{-3}	0.18	1.14	- 0.96
	$\sigma = 2$	-0.87×10^{-3}	0.33	1.43	- 1.30
	$\sigma = 5$	-0.79×10^{-3}	0.81	3.18	- 3.18
T_{yzz} ($mgal/km^2$)	$\sigma = 1$	-0.17×10^{-3}	0.28	1.06	- 1.15
	$\sigma = 2$	-0.21×10^{-3}	0.54	2.09	- 2.14
	$\sigma = 5$	-0.32×10^{-3}	1.35	5.18	- 5.33

Table 10. Statistics of Differences of

$$T_y - \left(\hat{T}_y + \Delta h\, \hat{T}_{yz} + \frac{1}{2}(\Delta h)^2 \hat{T}_{yzz}\right)$$

unit mgal

noise level (E)	mean	RMS	max	min
$\sigma = 1$	0.11	0.79	4.52	- 5.86
$\sigma = 2$	0.11	1.38	5.55	- 6.07
$\sigma = 3$	0.12	3.27	12.54	-12.81

Table 11. Statistics of Differences of

$$T_y - \left(\hat{T}_y + \Delta h\, \hat{T}_{yz}\right)$$

unit mgal

noise level (E)	mean	RMS	max	min
$\sigma = 1$	0.11	0.65	5.02	- 7.21
$\sigma = 2$	0.12	0.89	5.42	- 7.25
$\sigma = 5$	0.13	1.85	6.99	- 8.19

From Tables 4-11 we come to the following conclusion: The gravity disturbance can be determined on the earth's surface with demanded accuracy. With 1 Eötvös error in the gradient data, the components of the gravity disturbance T_x, T_y and T_z are determined with an accuracy in 1 mgal. Even though the measurement error is 5 E., the gravity disturbance can be determined with an accuracy of 3 mgal on the topographic surface.

Here we need to point out that the measurement error model is assumed a normal distributed random noise. Although this assumption is not entirely realistic it gives the main property of the effects of the error in the processing of the gradient data. It is expected that if the spectral

distributions of the gradient data and the measurement error are known, one can use the methods proposed in this study to minimize the effect of the measurement error and to get a stable and reasonable solution.

Normally, for a convergent series, the more correction terms that are taken, the results are determined more accurately. But we do not know whether the Taylor's series is convergent on the mean elevation level. From Tables 4-11 we can see that the correction term $1/2(\Delta h)^2 T_{zzz}$ may have some contribution to the large values of the gravity disturbance when the measurement error is small. But it supplies wrong information when the data accuracy is poor. Therefore we suggest if the area is very rough and the data are accurate enough, e.g. measurement error is lower than 1 E., then the correction term $1/2(\Delta h)^2 T_{zzz}$, etc., could be taken into account; in a flat area this term is very small and can be neglected; if the accuracy of the gradient data are poor, the correction term $1/2(\Delta h)^2 T_{zzz}$, etc., could be wrong and it is not of benefit to the results.

8. Conclusion

After many years of development the airborne gravity gradiometer survey system is coming in to practical application. Recently, a test flight was taken in the Texas-Oklahoma area which is characterized by a very smooth topography. Although this was the first time the gravity gradiometer survey system was flown, and only a fraction of the total runs yielded good gradient data, the components of the gravity disturbance were determined on the ground with the accuracy of 2 to 3 mgal in 5′ x 5′ mean anomalies.

In the future the test will be carried out in the rough mountain area and the topographic effect has to be taken into account. This problem has been considered by many authors. Tziavos et. al, have developed an estimation algorithms for the computation of the effect of the mass above the ellipsoid (Tziavos, et al., 1988). If we subtract the contribution of the topography from the gradient data, it means the mass of the earth is adjusted by removing the mass above the ellipsoid. This is not correct in some cases, e.g. the determination of the geoid. This report did not discuss this problem. Our goal was the determination of the gravity disturbance on the earth's surface. We assumed that the disturbing potential and its derivatives can be analytically downward continued to a mean level - in the report the mean elevation level was chosen, then the Taylor series was used. The gravity disturbance was given by (cf. Figure 1):

$$T_z(Q) = T_z(P') + \Delta h\, T_{zz}(P') + \frac{1}{2}(\Delta h)^2 T_{zzz}(P') \tag{9}$$

Obviously this analytical downward continuation problem is an improperly posed problem. The solution T_z (Q) may pose serious numerical difficult and not be stable.

For an improperly posed problem there are three methods that can be used: the least squares collocation, regularization and smoothing. How can they be used in the gravity gradiometry was studied in Section 3, 4 and 5. The studies indicate that the three methods are essentially the same. They filter out the high frequencies of the data and make the results smooth and stable. In comparison to the least squares collocation the methods of the regularization and smoothing are more flexible.

The regularization was used for a simulated computation. The numerical computation shows that this method is qualified for the analytical continuation of the derivatives of the disturbing potential, such as T_z, T_{zz}, T_{zzz} to the mean elevation level. When the accuracy of the gradient data was 1 Eötvös, the gravity disturbance was recovered with the accuracy of 1 mgal. If the accuracy of the gradient data is poor, but the ratio of the signal/noise is still high enough, the recovery of the

gravity disturbance can achieve a reasonable accuracy. One example described in the report is when the gravity disturbance was determined with an accuracy of 3 mgal when the accuracy of the gravity gradient data was 5 Eötvös.

The derivatives of the disturbing potential T_{zzz} can be obtained by processing the aerial gradient data but it is corrupted by the measurement errors. It is still a difficult work to get the higher derivatives of the disturbing potential and sometimes it looks like it is impossible. Fortunately the high derivatives of the disturbing potential have most effects on the high frequencies of the disturbing potential which do not have significant contribution to the disturbing potential.

For a flat area the first two terms in eq. (9) satisfied our needs, but in a rough mountain area the last term in (9) has to be considered if the accuracy of the gravity gradient data is high. If the accuracy of the gravity gradient data is poor, the last term is not beneficial to the results.

The numerical simulation was limited by different assumptions, such as the measurement error model, no position errors in the data, etc., but it represents the main property of the processing of the aerial gradient data and approximates the real world to a great extent. All the computations were completed by using the fast Fourier transformation.

References

Bachman, G.,and L. Narici, Functional Analysis, Academic Press, New York and London, 1966.

Bendat, J., A.G. Piersol, Engineering Applications of Correlation and Spectral Analysis, A. Wiley-Interscience Publication, John Wiley & Sons, 1980.

Brzezowski, S., D. Gleason, J. Goldstein, W. Heller, C., Jekeli, J. White, The Gravity Gradiometer Survey System and Test Results, in: Chapman Conference on progress in the Determination of the Earth's Gravity Field, 1988.

Chinnery, M.A., Terrain Corrections for Airbone Gravity Gradient Measurements, Geophysics, 26, 480-489, 1961.

Dorman, L.M. and B.T.R. Lewis, The Use of Non-linear Functional Expansions in Calculation of the Terrain Effect in Airborne and Marine Gravimetry and Gradiometry, Geophysics, 39, 33-38, 1974.

Gleason, D.M., Computing any Arbitrary Downward Continuation Kernel Function of an Integral Predictor Yielding Surface Gravity Disturbance Components from Airborne Gradient Data, manuscripta geodaetica, 13, 147-155, 1988.

Hammer, S., Topographic Corrections for Gradients in Airborne Gravimetry, Geophysics, 41, 346-352, 1976.

Heiskanen, W.A. and H. Moritz, Physical Geodesy, W.H. Freeman, San Francisco, 1967.

Ilk, K.H., Untersuchungen Zum Einfluss von a-priori Varianz-Kovarianzmatrizon anf die Lösung von Regularisierten Ausgleichungs problemen. In: Festschrift Rudolf Sigl zum 60. Geburtstag, Deutsche geodätische Kommission bei der Bayerischen Akademie der Wissenschaften, Reihe B, Heft Nr. 287, München, 1988.

Jekeli, C., On Optimal Estimation of Gravity From Gravity Gradients at Aircraft Altitude, Reviews of Geophysics, Vol. 23, No. 3, 1985.

Jekeli, C., Estimation of Gravity Disturbance Differences from a Large and Densely Spaced Heterogeneous Gradient Data Set Using an Integral Formula, manuscripta geodaetica, vol. 11, 48-56, 1986.

Jekeli, C., The Downward Continuation of Aerial Gravimetric Data Without Density Hypothesis, Bulletin Geodesique, 61, 319-329, 1987.

Miklin, S.G., Multidimensional Singular Integrals and Integral equations, Pergamon Press, Ltd., Headington, Hill Hall, Oxford, London, 1965.

Moritz, H., Advanced Physical Geodesy, Abacus Press, Tumbridge Wells, Kent, 1980.

Nashed, M.Z., Approximate Regularized Solutions to Improperly Posed Linear Integral and Operator Equations, in: Constructive and Computational Methods for Integral and Differential Equations, Lecture Notes in Mathematics, 430, 289-332, 1974.

Neyman, Y.M., Improperly Posed Problems in Geodesy and Methods of Their Solution, Proceedings of International Summer School on Local Gravity Field Approximation, 1985.

Rapp, R.H., S. Zhao, The 4 km x 4 km Free-Air Anomaly File for the Conterminous United States, Internal Report, Dept. of Geodetic Science and Surveying, The Ohio State University, 1988.

Rummel, R., K.P. Schwarz., M. Gerstl, Least Squares Collocations and Regularization, Bulletin Geodesique, 53, 343-361, 1979.

Schwarz, K.P., Geodetic Improperly Posed Problems and Their Regularization, Boll. Geod., e Sci. Affini, 38, p. 389-416, 1979.

Schwarz, K.P., M.G. Sideris, R. Forsberg, The Use of FFT Techniques in Physical Geodesy, Submitted to Geophysical Journal, 1989.

Sünkel, H., Die Darstellung Geodätischer Integral formula Durch Bikubische Spline-Funktionen, Mitterlungen der Geodätischen Institute der Technischen Universität Graz, Folge 28, Graz, 1977.

Tikonov, A.N., Regularization of Incorrectly Posed Problems, Soviet Math, Dokl., 4, 1624-1627, 1963.

Tziavos, I.N., M.G. Sideris, R. Forsberg, and K.P. Schwarz, The Effect of the Terrain Correction on Airborne Gravity and Gradiometry, Journal of Geophysical Research, Vol. 93, No. 138, 9173-9186, 1988.

Vassiliou, A.A., Numerical Techniques for Processing Airborne Gradiometer Data, Department of Surveying Engineering Report Numer 20017, University of Calgary, Calgary, Alberta, Canada, May, 1986.

Wang, Y.M., Problem der Glätting bei den Integraloperatoren in der Physikalischen Geodäsie, Doctoral Dissertation, Technical University, Graz, 1986.

Wang, Y.M., Numerical Aspects of the Solution of Molodensky's Problem by Analytical Continuation, manuscripta geodaetica, 12, 290-295, 1987.